

Multi-granularity Spatiotemporal Flow Patterns

Chrysanthi Kosyfaki^{1*}, Nikos Mamoulis², Reynold Cheng³,
Ben Kao³

^{1*}Department of Computer Science and Engineering, Hong Kong
University of Science and Technology, Hong Kong, China.

²Department of Computer Science and Engineering, University of
Ioannina, Ioannina, Greece.

³Department of Computer Science, University of Hong Kong, Hong
Kong, China.

*Corresponding author(s). E-mail(s): ckosyfaki@cse.ust.hk;

Contributing authors: nikos@cs.uoi.gr; ckcheng@cs.hku.hk;
kao@cs.hku.hk;

Abstract

Analyzing flow of objects or data at different granularities of space and time can unveil interesting insights or trends. For example, transportation companies, by aggregating passenger travel data (e.g., counting passengers traveling from one region to another), can analyze movement behavior. In this paper, we study the problem of finding important trends in passenger movements between regions at different granularities. We define Origin (O), Destination (D), and Time (T) patterns (ODT patterns) and propose a bottom-up algorithm that enumerates them. We suggest and employ optimizations that greatly reduce the search space and the computational cost of pattern enumeration. We also propose pattern variants (constrained patterns and top- k patterns) that could be useful to different applications scenarios. Finally, we propose an approximate solution that fast identifies ODT patterns of specific sizes, following a generate-and-test approach. We evaluate the efficiency and effectiveness of our methods on three real datasets and showcase interesting ODT flow patterns in them.

Keywords: transportation networks, spatiotemporal patterns, flow, pattern enumeration

1 Introduction

In a transportation network, nodes represent stations (or districts) and edges model the connections between the nodes carrying information related to movement or flow (e.g., passengers travel between districts during different times of a day). Examples include car or taxi passengers moving from one district of a city to another, metro or railway passengers, global travellers by air, etc. Transportation companies and organizations collect large volumes of data from their passengers, regarding their origins, destinations, and times of their trips. For each individual trip, the available information is typically the starting (or entry) location (or station) and time of the trip and the final (or exit) location (or station) and time. In-between locations (i.e., the entire trajectories) are often unavailable due to incapability of tracing and privacy constraints. For example, passengers of a metro network use their travel or credit cards at the entry and exit points of their trips and in-between locations can only be inferred. Similarly, taxi companies usually report the starting and ending locations (or districts) of trips instead of the entire trajectories.

Information on individual trips can be used in personalized services, after obtaining consent from the passengers. Other than that, it is hard to use such detailed data, mainly due to privacy constraints. However, aggregate information about passenger trips can be invaluable to the company since it can provide time-parameterized estimates and predictions about the passenger flow between regions, which can help to improve their service.

Problem We propose a novel analysis tool for transportation data, called *Origin-Destination-Time* (ODT) patterns. An ODT pattern captures information about the origins, destinations, and the volume (flow) of the passengers at different times of the day where the trips take place. We first use the application domain to define the finest granularity of regions on the map (e.g., each region corresponds to a metro station or a district) and also define the finest time intervals of interest (e.g., divide the 24-hour time interval of a day into 48 equal 30-minute timeslots or use short slots at peak hours and long ones at night). We call these *atomic regions* and *atomic timeslots*, respectively. This means that, a trip can be described by its origin region, its destination region, and the timeslot when the trip starts, i.e., as an (o, d, t) triple. For all (o, d, t) triples, where o and d are (different) atomic regions and t is an atomic timeslot, we measure the total number of passengers who took a trip from o to d at time t . The total flow of an (o, d, t) triple characterizes its importance; the triples with high flow are considered to be important and they are called *atomic ODT-patterns* (we drop the ODT prefix whenever the context is clear). In a *generalized* ODT-triple, denoted by (O, D, T) , O and D are sets of *neighboring* atomic regions and T consists of one or more *consecutive* timeslots. An atomic (o, d, t) triple is a component of an (O, D, T) triple if $o \in O$, $d \in D$, and $t \in T$. (O, D, T) is *non-atomic*, if at least one of O , D , or T is non-atomic. Figure 1 exemplifies a generalized ODT pattern, which captures statistically significant movement in Brooklyn from boroughs $\{35,77,177\}$ to boroughs $\{25,40,106\}$ in the mornings of weekdays.

Methodology The number of possible atomic region combinations that can form a generalized (i.e., non-atomic) region O or D is huge and it is not practical to consider

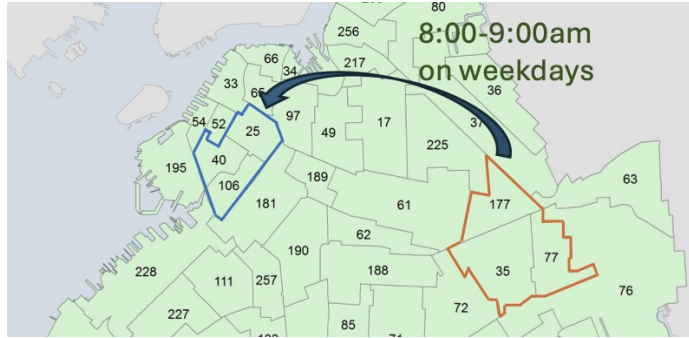


Fig. 1: Example of an ODT pattern

all these combinations and their flows. At the same time, for a given generalized ODT triple, it is hard to estimate the flow quantity that can be deemed significant enough to characterize the triple an interesting pattern. To solve these issues, we follow a *voting* approach, where we characterize an ODT triple as a pattern if at least a certain percentage of its constituent (o, d, t) triples are atomic patterns (i.e., they have large enough flow). This allows us to design and use a pattern enumeration algorithm, which, starting from the atomic patterns, identifies all ODT patterns progressively by synthesizing them from less generalized ODT patterns. We propose a number of optimizations, which significantly reduce the time spent for generating candidate patterns and measuring their significance.

Problem variants Given the potentially large number of ODT patterns and the high cost of their enumeration, we also study practical ODT variants. First, we investigate the detection of patterns which are *constrained* to a subset of regions and timeslots, allowing us to focus on under-represented regions and to greatly reduce the pattern enumeration cost. Second, we study pattern detection by limiting the number of atomic regions and timeslots that a pattern may have. Finally, we define and solve the problem of finding the top-ranked patterns at each granularity level, by a novel algorithm that significantly outperforms the baseline approach of finding all patterns at each level and then selecting the top ones.

Approximate algorithms In this paper, our primary focus shifts in addressing the computational challenges of enumerating ODT patterns [1]. As we mention earlier, enumerating all the possible ODT triples makes exhaustive enumeration computational prohibitive. To further accelerate the enumeration of generalized ODT patterns, we propose an approximate solution that significantly reduces both space and time complexity compared to the baseline algorithm. Assuming that we are interested in ODT patterns, where the O, D, and T components have specific sizes (e.g., O consists of 4 neighboring districts), we first generate three pools of O-candidates, D-candidates and T-candidates. O-candidates and D-candidates are connected subgraphs in the region neighborhood graph, which have the requested sizes. T-candidates are sequences of consecutive timeslots of the requested size (e.g., 2-hour periods). Our approximate

algorithm follows a generate-and-test approach, which samples triples of ODT combinations from the candidates and counts whether they include a sufficient number of atomic patterns. To improve the effectiveness of our approximate algorithm, we also propose a weighted version, which tests the most promising ODT combinations to become ODT patterns.

Applications The problem of identifying ODT patterns finds application in a wide variety of real-world transportation networks [2–4], such as road networks, railways, etc. For example, passenger movement patterns can facilitate the handling of emergencies or incidents by metro systems. Consider an accident that happened in Hong Kong subway system in December 2021¹. Scheduled trips from some districts were cancelled and passengers had to be served by other means (i.e., buses). ODT patterns could help to schedule on-demand transportation for affected passengers as they could indicate origin-destination region pairs served by the disrupted route with heavy demand at the time of the day when the incident happened. In general, ODT patterns can help transportation companies to improve their schedule and in managing their available resources (e.g., fleet, employees). Another application is identifying the correlation between map districts for performing target-marketing, cross-district advertisements, or location planning. For example, if there is a heavy passenger flow between districts that are far from each other, the municipality may consider allocating new space for housing or opening new services near the residencies of passengers, to reduce traffic and improve the environmental conditions.

Novelty The input to our problem are not the entire trajectories of passengers, which is typically not available to transportation companies or organizations, as already discussed. Instead, we assume that we only have access to the (anonymized) trips of passengers, either individually or aggregated (e.g., the total number of passengers who took a trip from a specific origin to a specific destination at a specific time). For example, metro companies only have access to the entry and exit points of passengers, whereas public taxi trip data only include the origin/destination districts and time of the trip, but not the route. Hence, sequence or trajectory data mining methods are not applicable to our problem. In addition, our goal is also very different compared to the objective of sequence pattern mining. We study the identification of frequent generalized ODT triples, where the origins, destinations, and timeslots could be generalized to be a subgraph of neighboring regions or a time interval. On the other hand, the goal of sequence/trajectory mining methods is to find frequent subsequences. Table 1 summarizes representative works on traffic flow mining (TFM), sequential and trajectory pattern mining (STM), origin-destination flow prediction (ODFP), and travel time estimation (TTE) problems and their differences compared to our work. In summary, all works consider time, but ours is the only work that (i) finds generalized ODT patterns, (ii) does not require in-between points of trajectories, and (iii) considers flow in pattern detection. For a detailed comparison to previous work, see Sec. 2.

Outline Section 2 reviews related work on spatio-temporal pattern mining. In Section 3, we formally define the problem we study in this paper. Section 4 presents an algorithm for extracting spatio-temporal flow patterns and its optimizations. In Section 5,

¹[https://www.thestandard.com.hk/breaking-news/section/4/183861/\(Video\)-MTR-door-flew-off,-disrupting-peak-hour-service](https://www.thestandard.com.hk/breaking-news/section/4/183861/(Video)-MTR-door-flew-off,-disrupting-peak-hour-service)

Table 1: Previous works

| Previous works | Characteristics | | | | |
|----------------------------------|-----------------|----------------|------|---------------|------|
| | ODT | Generalization | Time | Req. Traject. | Flow |
| TFM ([2, 5–7]) | | ✗ | ✓ | ✗ | ✓ |
| STM ([8–14]) | | ✗ | ✓ | ✓ | ✗ |
| ODFP ([3, 15–19]) | | ✗ | ✓ | ✗ | ✓ |
| TTE ([20–23]) | | ✗ | ✓ | ✓ | ✗ |
| ODT patterns ([our work]) | | ✓ | ✓ | ✗ | ✓ |

we define interesting variants of flow patterns and propose algorithms for their enumeration. In Section 6, we propose an approximate method which generates components of ODT patterns which participate in many atomic patterns and tests combinations of them to identify potential patterns. Section 7 evaluates our methods on real networks with different characteristics. Finally, Section 8 concludes the paper with a discussion about future work.

2 Related Work

The problem of enumerating, counting, and identifying spatiotemporal patterns has been studied for over three decades, reflecting its importance in data mining and in general in urban analytics [6, 16, 24–59]. The main goal of the problem is as follows: Given a graph G , identify spatial events, correlations, or sequences that recur over time. Despite considerable progress, existing methods still face challenges in computational efficiency and scalability. The high computational cost of current approaches has pushed researchers to explore alternative problem formulations and faster algorithms. There is also a practical need for methods that work with minimal input parameters (e.g., a trajectory cannot be available due to privacy constraints) while extracting useful patterns. Managing efficiency with pattern quality under minimal user specification remains an open challenge. In this section, we review works across several related areas: sequential pattern mining, trajectory pattern mining, traffic flow analysis, travel time estimations, and origin-destination flow prediction. These areas provide context for our approach and highlight current methods for discovering spatiotemporal patterns.

Sequential and Trajectory Pattern Mining Sequential pattern mining methods [24, 60] discover interesting subsequences, based on occurrence frequency. Agrawal and Srikant [8] introduced the concept of sequential item-purchase patterns over a database of time-ordered customer transactions. Similar to sequence mining, trajectory pattern mining is the problem of identifying frequent subsequences in space and time [10, 13, 14, 61, 62]. Spatio-temporal patterns are discovered from raw GPS data, which capture routes or passenger movements. Giannotti et al. [12] suggested the discovery of regions of interest in trajectory pattern mining, as considering sequences of predefined regions reduces the complexity of the problem. In the same spirit, Cao et al. [60] automatically segment the space into spatial regions by clustering the tracked object locations; then, they identify sequential patterns of regions that repeat themselves over time. Choi et al., [63] introduce a tool for discovering all regional movement patterns in semantic trajectories. In a semantic trajectory [9], each point of a trajectory not only represents

a specific location but also contains a semantic category. Patterns can then be defined based on semantics and locations over time. Fan et al. [11] propose scalable trajectory mining methods using Spark.

Our problem is very different compared to previous work on trajectory, sequence, and graph mining. First, we are not interested in finding frequent paths (subsequences, subgraphs), but in finding hot combinations of trip origins, destinations, and timeslots. Second, we do not search for patterns at the finest granularity only, but looking for patterns where any of the three ODT components are generalized at an arbitrary granularity. Furthermore, we only use a *weak monotonicity* property to construct and validate generalized patterns from more detailed ones, which means that the classic Apriori algorithm (and its variants) [64–68] cannot be readily applied to solve our problem.

Traffic Flow Mining Mining traffic flow patterns [2, 5–7] is another related problem to ODT patterns. Liu et al. [2] studied the problem of extracting traffic flow knowledge from transportation data, i.e., pairs of POIs on the map that have significant traffic flow between them. Although we also measure flow between regions, none of these previous works studies flow patterns at *different granularities*, where regions and time periods may consist of multiple atomic elements; hence, previous works cannot be applied to solve our problem. Moreover, they require in-between locations, which may not be available and are not relevant to our problem’s objective.

Travel Time Estimation The main objective of *Travel Time Estimation (TTE)* is to estimate the time to travel from a specific origin location on the map to a specific destination at a given time [20, 22, 23]. Lin et al., [21] propose an indexing approach (oracle) for estimating the travel time between different regions at different times of the day. Although they also use the term *ODT*, our goals are completely different. While our main objective is to identify (generalized) Origin-Destination-Time patterns considering the (passenger) flow, their goal is to predict the travel time from a specific detailed region O to a detailed destination D at a time T .

Origin-Destination Flow Prediction Predicting the origin-destination traffic flow has been a well-studied problem in transportation research [3, 15–19, 59, 69–74]. The main objective is to estimate the flow (e.g., number of passengers in a transportation network or cars in a road network) between origin-destination pairs. A typical approach is to construct a Origin-Destination matrix [75], where each cell represents the trips between an origin and a destination. Tu et al., [48] study the stability of travel patterns on different times of the day and use predefined geographic units to group the origin-destination pairs of each journey. Behara et al., [16] study the problem of OD flow prediction by proposing a geographical window-based structural similarity (GSSI) index that captures statistics of geographically correlated OD pairs. OD pairs correlate if they share similar structural properties and therefore expand to neighbor regions. Their proposed solution can help identifying local patterns more efficiently. Similarly, [59] proposes a DBSCAN framework to identify travel patterns in multi-density high dimensional matrices. Although [16, 59] share similarities with our work, the set up of the problem is different. First, they use similarity metrics to group regions together when defining OD pairs. In our

case, we perform region and time generalization based on (geographic) adjacency and connectivity in a neighborhood graph. Wang et al., [3] develop a model for predicting the flow density in different origin-destination pairs. To this end, they represent a city as a grid and take into consideration regions that may have a significant amount of flow compared to other less important regions. The goal of this work is similar to ours, however they use additional data such as POIs and area proximity, which, in our case, are not available. In summary, our framework can identify flow patterns that can be used to predict demands in the flow between generalized regions and at (generalized) timeslots efficiently using the minimum available information.

3 Definitions

In this section, we formally define ODT patterns and the graph wherein they are identified. Table 2 shows the notations used frequently in the paper.

Table 2: Table of notations

| Notations | Description |
|-------------------------------------|--|
| $G(V, E)$ | region neighborhood graph |
| r_i | atomic region |
| R_i | region |
| t_i | atomic timeslot |
| T_i | timeslot |
| P | atomic ODT pattern or triple |
| $P.O$ | pattern/triple origin |
| D | pattern/triple destination |
| T | pattern/triple timeslot |
| $\sigma(P)$ | support of atomic ODT pattern P |
| s_a | support of atomic regions and timeslots |
| s_r | ratio threshold |
| $P.cnt$ | number of atomic patterns in ODT pattern P |
| $\mathcal{P}_\ell/\mathcal{T}_\ell$ | Set of ODT patterns/triples at level ℓ |

The main input to our problem is a *trips* table, which records information about trips from origins to destinations at different times. Each origin/destination is a minimal region of interest on a map (e.g., a district, a metro station, etc.), called *atomic region*. Atomic regions are specified by the application; they could be pre-defined districts or stations/stops and their nearby area. Spatial clustering can also be applied on precise locations (e.g., taxi pickup/dropoff locations) to define a set of atomic regions, as in [60]. Let V be the set of all atomic regions. An undirected graph $G(V, E)$ defines the neighboring relations between atomic regions; there is an edge (v, u) in E iff $v \in V$ and $u \in V$ are neighbors on the map. Finally, the timeline is divided into periods that repeat themselves (e.g., 24-hours each) and each period is discretized into time ranges (e.g., 48 30-minute slots). Discretization of time can be uniform or it may follow the data distribution (e.g., using the boundaries of an equi-depth histogram). Each minimal time range of interest is called *atomic timeslot*. Periods can also be classified (e.g., weekdays vs. weekends); hence atomic timeslots may refer to different period classes (e.g., 8:00-8:30 on weekdays).

Definition 1 (Region/Timeslot) A region r is a subset V' of V , such that the induced subgraph $G'(V', E')$ of G is connected. A timeslot T is a continuous sequence of atomic timeslots.

Definition 2 (Generalization of a region/timeslot) A region R_1 is a generalization of region R_2 iff $R_2 \subset R_1$. A timeslot T_1 is a generalization of timeslot T_2 iff $T_2 \subset T_1$.

Definition 3 (Minimal generalization of a region/timeslot) A region R_1 is a minimal generalization of region R_2 iff $R_2 \subset R_1$ and $R_1 - R_2$ is an atomic region. A timeslot T_1 is a minimal generalization of timeslot T_2 iff $T_2 \subset T_1$ and $T_1 - T_2$ is an atomic timeslot.

For example, region $\{B, C, D\}$ is a minimal generalization of $\{B, D\}$. Symmetrically, $\{B, D\}$ is a minimal specialization of $\{B, C, D\}$.

We found that the start and end times of individual trips between the same origin and destination are strongly correlated. Hence, we can map each trip in the trips table to an *atomic ODT triple* (o, d, t) , where o is the origin region of the trip (GPS locations can be mapped to the nearest spatially $v \in V$), d is the trip's destination region, and t is the atomic timeslot that contains the trip's origin time.²

Definition 4 (Atomic ODT triple) A triple (o, d, t) is atomic if:

- o is an atomic region
- d is an atomic region
- t is an atomic timeslot
- $o \neq d$

Given an atomic ODT triple P , the *support* $\sigma(P)$ of P is the total number of passengers (flow) of the trips that are mapped to P . For example, the top-left of Figure 2 shows a map and an individual trip in it. The top-right of Figure 2 has the *aggregated trips table*, which contains all atomic (o, d, t) triples, after aggregating all trips that correspond to the same (o, d, t) . For instance, trips $(B, D, 9:20, 2)$ and $(B, D, 9:29, 1)$ are merged to triple $(B, D, 18)$ with total flow 3.³ Next, we define generalized (i.e., non-atomic) ODT triples.

Definition 5 (ODT triple) An ODT triple (O, D, T) consists of a region O , a region D , and a timeslot T , such that $O \cap D = \emptyset$.

Definition 6 (ODT triple generalization) An ODT triple P_1 is a generalization of ODT triple P_2 if for each $X \in \{O, D, T\}$, either $P_1.X = P_2.X$ or $P_2.X \subset P_1.X$, and for at least one $X \in \{O, D, T\}$, $P_2.X \subset P_1.X$.

²Our definitions and techniques can be extended for data inputs where there is no correlations between the begin and end times of trips; in this case, we should map trips to (o, d, st, et) quadruples and patterns should be ODSE quadruples.

³All time moments between 9:00 and 9:30 are generalized to timeslot 18, which is the 18th slot in 30-minute intervals, starting from 00:00-00:30 (mapped to 0).

Definition 7 (Minimal generalization of ODT triple) An ODT triple P_1 is a minimal generalization of ODT triple P_2 if one of the following holds:

- $P_1.O = P_2.O$, $P_1.D = P_2.D$ and $P_1.T$ is a minimal generalization of $P_2.T$
- $P_1.D = P_2.D$, $P_1.T = P_2.T$ and $P_1.O$ is a minimal generalization of $P_2.O$
- $P_1.O = P_2.O$, $P_1.T = P_2.T$ and $P_1.D$ is a minimal generalization of $P_2.D$

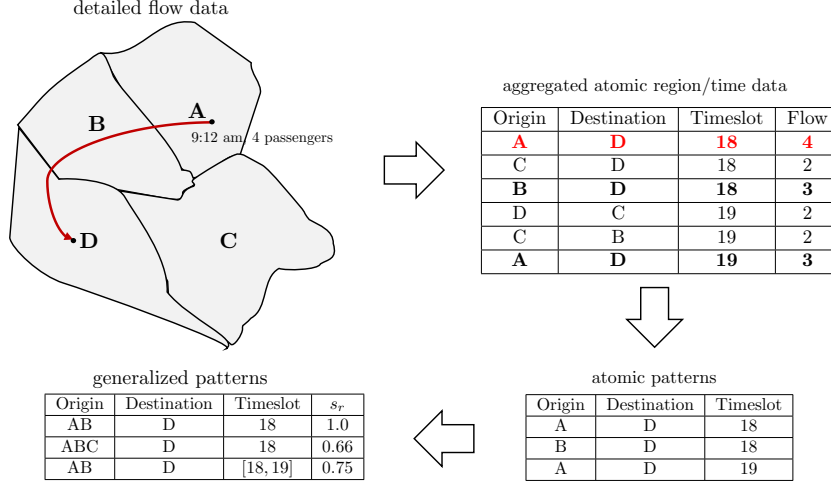


Fig. 2: A detailed example

We now turn to the definition of ODT patterns; we start by atomic ODT patterns and then move to the generalized ODT patterns.

Definition 8 (Atomic ODT pattern) Let AT_r be the set of atomic ODT triples with non-zero support. Given a threshold s_a , $0 < s_a \leq 1$, an atomic ODT triple P is called an atomic ODT pattern if $\sigma(P)$ is in the top $s_a \times |AT_r|$ supports of triples in AT_r .

The rationale of using s_a is that we want to restrict the set of important atomic ODT triples, by considering as patterns the triples that have large total flow (accumulated over the repeated instances of the triples in the trips table). Figure 2 (bottom-right) shows the atomic ODT patterns for our running example if $s_a = 0.5$.

Definition 9 (ODT pattern) An ODT pattern P is an ODT triple where:

- the ratio of atomic triples in P , which are atomic patterns, is at least equal to a *minimum ratio* threshold s_r
- there exists a minimal specialization of P , which is an ODT pattern

The number of atomic triples in P , which are atomic patterns is denoted by $P.\text{cnt}$. In the example of Figure 2, if $s_r = 0.6$, $(AB, D, 18)$ is a (generalized) ODT pattern where origins A and B have significant joint flow to destination D at timeslot $t = 18$, because the pattern includes two out of three atomic patterns. The second condition of Definition 9 is a *sanity* constraint, which prevents a generalized triple P from being characterized as a pattern if there is no minimal specialization of P that is also a pattern; intuitively, a pattern should have at least one minimal specialization which is also a pattern (weak monotonicity).

A pattern (triple) P is said to be level- ℓ pattern (triple) if the total number of atomic elements in it (regions and timeslots) is ℓ . Hence, atomic patterns are level-3 patterns, since they contain exactly 3 elements (i.e., two atomic regions and one atomic timeslot). Similarly, triple $(A, BC, [1, 3])$ is a level-6 triple because it includes 1 atomic region in its origin, 2 atomic regions in its destination, and 3 atomic timeslots in its time-range (note that $[1, 3]$ includes atomic timeslots $\{1, 2, 3\}$).

4 Pattern extraction

To find the ODT patterns, we first start by finding the atomic ODT patterns, i.e., the (o, d, t) triples which are frequent/significant, where o and d are atomic regions and t is an atomic timeslot. This is trivial and can be done by one pass over the aggregated trips data, where the occurrence of each (o, d, t) triple is unique and by selecting the top s_a ratio of them as atomic patterns. Our most challenging task is then to define an algorithm that progressively synthesizes non-atomic patterns from atomic patterns and prunes the search space effectively.

Recall that a non-atomic triple $P = (O, D, T)$ is a pattern if at least a ratio $s_r > 0$ of its included atomic triples are patterns. Hence, by definition, a non-atomic pattern generalizes at least one atomic pattern (o, d, t) . The pattern synthesis algorithm uses the set of atomic patterns and the region neighborhood graph G to form the non-atomic patterns. Given an existing (O, D, T) pattern P , we attempt a minimal generalization of P by including into the set O a neighboring atomic region to the existing regions in O , or doing the same for set D , or adding an atomic neighboring timeslot to T .

The challenge is to prune candidate generalizations that cannot be patterns. For this, we need a fast way to compute (or bound) the number of contributing (newly added to P) atomic patterns to the ratio of the candidate.

4.1 Baseline Algorithm

We now present a baseline algorithm for enumerating all the atomic and extended ODT patterns in an input graph $G(V, E)$. The first step of Algorithm 1 is to scan all trips data and compute the support counts of all atomic triples \mathcal{T}_3 . Then, it finds the set \mathcal{P}_3 of atomic patterns, i.e., the triples having support count at least equal to minsup , which is the support count of the $s_a \cdot |\mathcal{T}_3|$ -th triple in \mathcal{T}_3 in decreasing support order. All triples (patterns) in \mathcal{T}_3 (\mathcal{P}_3) have exactly three atomic elements (regions or timeslots). The algorithm progressively finds the patterns with more atomic elements. Recall that a triple (pattern) P is at level ℓ , i.e., in set \mathcal{T}_ℓ (\mathcal{P}_ℓ) if it has ℓ atomic

elements; we also call P a level- ℓ triple (pattern). Candidate patterns $CandP$ at level $\ell + 1$ are generated by either adding an atomic region at O or an atomic region at D or an atomic timeslot at T , provided that the resulting triple is valid according to Definition 5. If a $CandP$ has been considered before, it is disregarded. This may happen because the same triple can be generated from two or more different triples at level ℓ . For example, candidate pattern $(AB, C, 1)$ could be generated by pattern $(A, C, 1)$ (by extending region A to region AB) and by $(B, C, 1)$ (by extending region B to region AB). Hence, we keep track at each level ℓ the set of triples that have been considered before, in order to avoid counting the same candidate twice.⁴

To check whether a candidate $CandP$ not considered before is a pattern, we need to divide the number $CandP.cnt$ of atomic patterns included in $CandP$ by the total number $CandP.card$ of atomic triples in $CandP$. If this ratio is at least s_r , then $CandP$ is a pattern. $CandP.card$ can be computed algebraically: it is the product of atomic number elements in each of the three ODT components. For example, $(AB, CD, [1, 3]).card = 2 \cdot 2 \cdot 3 = 12$ because there are 12 atomic triples in $(AB, CD, [1, 3])$, i.e., combinations of elements $\{A, B\}$, $\{C, D\}$, and $\{1, 2, 3\}$. To compute $CandP.cnt$ fast, we can take advantage of the fact that we already have $P.cnt$, i.e., the number of atomic patterns in the generator pattern. We only have to compute the $P'.cnt$ for the *difference* $P' = CandP - P$ between $CandP$ and P , which is the triple consisting of the extension element in the extended dimension (one of O, D, T) together with the element-sets in the intact dimensions (two of O, D, T). For example, if $P = (A, CD, [1, 2])$ and $CandP = (AB, CD, [1, 2])$, then $P' = (B, CD, [1, 2])$. To compute $P'.cnt$, Algorithm 1 enumerates all atomic triples in P' to check whether they are patterns. It then sums up $P.cnt$ and $P'.cnt$ to derive $CandP.cnt$.

Figure 3 exemplifies the pattern enumeration process in our running example (see Figure 2). Atomic pattern $P = (A, D, 18)$ can be generalized by adding to the origin any of the neighbors of atomic region A , to the destination any of the neighbors of atomic region D , and to timeslot 18 either timeslot 17 or timeslot 19. Each of these generalization forms a candidate pattern $CandP$ at level 4. Counting the support of these candidates requires counting only the difference P' . For example, to count the support of $(AB, D, 18)$, we only have to add to the support of $P = (A, D, 18)$ the support of $P' = (B, D, 18)$, which is 1. Then, the support of $(AB, D, 18)$ is found to be 2. Assuming that $s_r = 0.6$, $CandP = (AB, D, 18)$ is a pattern, since the ratio of atomic patterns in it is $1.0 \geq s_r$. All patterns that stem from $P = (A, D, 18)$ up to level 5 are emphasized in Figure 3; these are used to generate candidate patterns at the next levels.

Complexity Analysis In the worst case, all valid combinations of regions and timeslots can be considered as candidate patterns. In other words, each subset of V can be the union of O and D and for each such subset of size k can be split in $2^k - 2$ ways. Hence, the number of possible OD pairs is $\sum_{k=1}^{|V|-1} \binom{|V|}{k} (2^k - 2)$. If S is the number of atomic timeslots, then the number of possible (generalized) timeslots to be included

⁴Since a pattern at level $\ell + 1$ requires at least one and not all its minimal specializations to be patterns, an id-numbering scheme for atomic regions, which would extend patterns by only adding elements that have larger id would not work. For example, if both $(A, C, 1)$ and $(B, C, 1)$ are patterns, $(AB, C, 1)$ can be generated by both of them; however, if just $(B, C, 1)$ is a pattern, $(AB, C, 1)$ can only be generated by $(B, C, 1)$.

Algorithm 1 Baseline Algorithm for finding all ODT patterns

Require: a region graph $G(V, E)$; a trips table; a minimum support s_a for atomic ODT patterns; a minimum support ratio s_r for non-atomic ODT patterns

- 1: \mathcal{T}_3 = atomic triples computed from trips table
- 2: \mathcal{P}_3 = triples in \mathcal{T}_3 with support $\geq s_a \times |\mathcal{T}_3|$
- 3: **for** all atomic triples $P \in \mathcal{T}_3$ **do**
- 4: $P.\text{cnt} = 1$ if $P \in \mathcal{P}_3$, else $P.\text{cnt} = 0$
- 5: **end for**
- 6: $\ell = 3$
- 7: **while** $|\mathcal{P}_\ell| > 0$ **do** $\triangleright \mathcal{P}_\ell$ = set of level- ℓ patterns
- 8: $\mathcal{P}_{\ell+1} = \emptyset$ \triangleright Initialize pattern set at level $\ell + 1$
- 9: **for** each P in \mathcal{P}_ℓ **do**
- 10: **for** each minimal generalization CandP of P **do**
- 11: **if** CandP not considered before **then**
- 12: $P' = \text{CandP} - P$
- 13: $\text{CandP}.\text{cnt} = P.\text{cnt} + P'.\text{cnt}$
- 14: **if** $\text{CandP}.\text{cnt} / \text{CandP}.\text{card} \geq s_r$ **then**
- 15: add CandP to $\mathcal{P}_{\ell+1}$
- 16: **end if**
- 17: **end if**
- 18: **end for**
- 19: **end for**
- 20: $\ell = \ell + 1$
- 21: **end while**

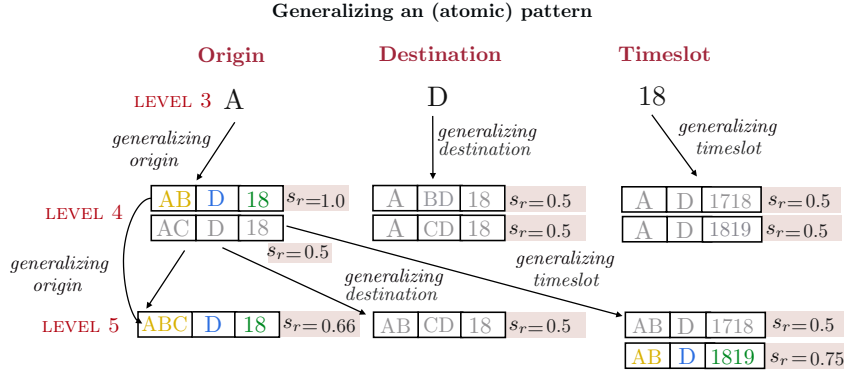


Fig. 3: Pattern enumeration example

in a candidate pattern is $2^{|S|}$. Hence, the worst-case space/time complexity of ODT pattern enumeration is $O\left(2^{|S|} \sum_{k=1}^{|V|-1} \binom{|V|}{k} (2^k - 2)\right)$.

4.2 Optimizations

We now discuss some optimizations to the baseline algorithm, which can greatly enhance its performance in practice.

Avoid re-counting P' . The first approach is based on *caching* the ODT triples that have been counted before. Instead of computing $P'.$ cnt directly for $P' = \text{CandP} - P$, we first check whether $P'.$ cnt is already available. This requires us to cache the counted triples and their supports at each level in a hash table. Hence, before counting

P' , we first search the hash table, which caches the triples at level $|P'|$ to see if P' is in there. In this case, we simply use $P'.cnt$ instead of computing it again from scratch.

Fast check for zero support of P' . The second optimization is based on the observation that for some pairs (o, d) of atomic regions, there does not exist any timeslot t , such that (o, d, t) is an atomic pattern in \mathcal{P}_3 . For example, if o and d are remote regions on the map, it is unlikely that there is significant passenger flow that connects them at any time of the day. We take advantage of this to avoid counting any P' which may not include atomic patterns. Specifically, for each atomic region r , we record (i) $r.dests$, the set of atomic regions r' , such that there exists a (r, r', t) pattern in \mathcal{P}_3 ; and (ii) $r.srcs$, the set of atomic regions r' , such that there exists a (r', r, t) pattern in \mathcal{P}_3 . If, in Algorithm 1, $CandP$ is a minimal generalization of P , by expanding $P.O$ to include a new atomic region r , then $P' = CandP - P$ should only include r in $P'.O$. If $P'.D \cap r.dests = \emptyset$, then P' does not include any atomic patterns and $CandP.cnt$ is guaranteed to be equal to $P.cnt$. Hence, we can skip support computations for P' . Symmetrically, if $CandP$ is a minimal generalization of P , by expanding $P.D$ to include a new atomic region r , then $P' = CandP - P$ should only include r in $P'.D$. If $P'.O \cap r.srcs = \emptyset$, then $CandP.cnt$ is guaranteed to be equal to $P.cnt$. Overall, by keeping track of $r.dests$ and $r.srcs$ for each atomic region r , we can save computations when counting the supports of patterns. Since the space required to store $r.dests$ and $r.srcs$ is $O(|V|)$ in the worst case, the total space complexity of these sets is $O(|V|^2)$. This cost is bearable, because our problem typically applies on transportation networks or district neighborhood graphs in urban maps, where the number of vertices in V is rarely large.

Improved neighborhood computation. The minimal generalizations of a pattern P are generated by minimally generalizing $P.O$, $P.D$, and $P.T$. The generalization of $P.T$ is trivial as we add one atomic timeslot before the smallest one in $P.T$ or after the largest one in $P.T$. On the other hand, computing the minimal generalizations of a region R (i.e., $P.O$ or $P.D$) can be costly if done in a brute-force way. The naive algorithm tries to add to $P.O$ all possible neighbors of each atomic region $r \in R$ and for each such neighbor not in $P.O$ and $P.D$ it measures the support of the corresponding generalized pattern P' , if P' was not considered before. Since the same P' can be generated by multiple P , checking whether P' has been considered before can be performed a very large number of times with a negative effect in the runtime. We design a neighborhood computation technique for a region R , which avoids generating the same P' multiple times. The main idea is to collect first all neighbors of all $r \in R$ in a set N and then compute (in one step) $N - P.O - P.D$, i.e., the set of regions r that minimally expand R to form the minimal generalizations of P .

Indexing atomic patterns. As another optimization, we employ a prefix-sum index which can help us to compute an upper bound of the support of P' . The main idea comes from indexes used to compute range-sums in OLAP [76]. Let N be the number of atomic regions and M be the number of atomic timeslots. Consider a $N \times N \times M$ array A , where each cell corresponds to an atomic ODT triple. The cell includes a 1 if the corresponding atomic ODT triple is a pattern; otherwise the cell includes a 0. In addition, consider a 3D array R with shape $(N+1) \times (N+1) \times (M+1)$. Each element $R[i][j][k]$ of R is the sum of all elements $A[i'][j'][k']$ of A , such that

$i' \leq i, j' \leq j$, and $k' \leq k$ $R[i][j][k] = 0$ if any of i, j, k is 0. R is the *prefix-sum* array of A , as illustrated in Figure 4.

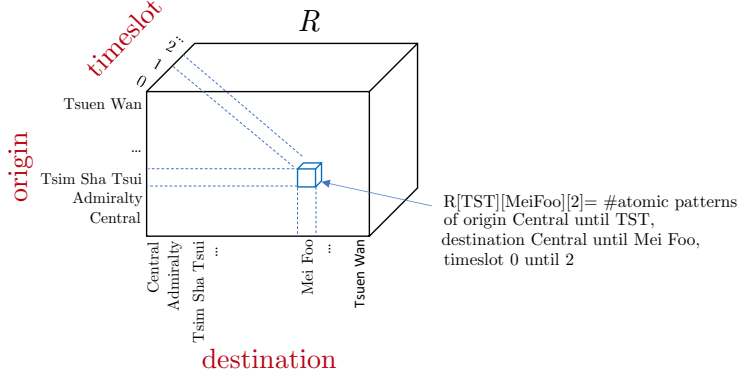


Fig. 4: Prefix sum example

Consider a 3D range $[a, b], [c, d], [e, f]$, where $0 < a \leq b \leq N, 0 < c \leq d \leq N$, and $0 < e \leq f \leq M$. The sum of values in A inside this range can be computed as follows:

$$\begin{aligned}
& R[b][d][f] \\
& - R[a-1][d][f] - R[b][c-1][f] - R[b][d][e-1] \\
& + R[a-1][c-1][f] + R[b][c-1][e-1] + R[a-1][d][e-1] \\
& - R[a-1][c-1][e-1]
\end{aligned}$$

Now, consider a P' which needs to be counted. P' includes a set of atomic origin regions, a set of atomic destination regions, and a set of atomic timeslots. The atomic timeslots are guaranteed to be a continuous sublist of regions in the corresponding dimension of the 3D array A , starting, say, from timeslot e and including up to timeslot f . However, the region sets in P' are not guaranteed to be continuous. Still, the 3D range $[a, b], [c, d], [e, f]$, where a (e) is the origin (destination) region in P' with the smallest ID and b (d) is the origin (destination) region in P' with the largest ID is guaranteed to be a superset of atomic triples in P' . Hence, the prefix-sum index can give us in $O(1)$ time an *upper bound* of the number of atomic patterns in P' . If this upper bound is added to the support of P and the resulting support is less than s_r , then $CandP$ is definitely not a pattern, so we can avoid counting P' . To maximize the effectiveness of this optimization, we give IDs to regions by applying a depth-first traversal of G from the vertex with the smallest degree.

5 Pattern Variants

In this section, we explore alternative problem definitions and the corresponding ODT pattern extraction algorithms that can be more useful than our general definition in certain problem instances. In particular, we observe that the number of patterns can be huge even if relatively small s_a and large s_r are used. In addition, setting global

thresholds may not be “fair” for some regions which are under-represented in the data. To address these issues, we propose (i) size-bounded patterns, (ii) constrained-pattern search, and (iii) rank-based patterns.

5.1 Size-bounded Patterns

The first type of constraint that we can put to limit the number of patterns is on the sizes of the pattern O , D , and T components. Specifically, we can set an upper bound B_O to the number of atomic regions in an origin region of a pattern. Similarly, we can limit the number of regions in D to at most B_D and the number of atomic timeslots to at most B_T . In effect, this limits the number of levels that we use for pattern search to $B_O \cdot B_D \cdot B_T$. For pattern enumeration, we use the same algorithms and optimizations discussed in Section 4, but with the constraints applied whenever we expand a pattern to generate the candidate patterns at the next level.

5.2 Constrained Patterns

Another way to control the number of the patterns, but also focus on specific regions and/or timeslots that are under-represented in the entire population is to limit the domain of atomic regions and timeslots. Specifically, we give as parameter to the problem the set of atomic regions $V_O \subseteq V$ that we are interested in to act as origins the set $V_D \subseteq V$ of regions that can act as destinations, and $T_R \subseteq T$, a restricted contiguous subsequence of the entire sequence of atomic timeslots T to be used as timeslots in the patterns. The induced subgraphs by V_O and V_D should be connected, in order to potentially have the entire V_O (and/or V_D) as an origin (destination) of a pattern. For example, if a data analyst is interested in flow patterns from South Manhattan to Queens in afternoon hours, she could include in V_O (resp. V_D) all the atomic regions in South Manhattan (resp. Queens) and restrict the timeslots to be used in patterns to only afternoon hours. Depending on the sizes of V_O , V_D , and T_R pattern enumeration can be significantly faster compared to unconstrained pattern search.

5.3 Rank-based patterns

Another way to control the number of patterns and still not miss the most important ones is to regard as patterns, at each level, the k triples with the highest support and prune the rest of them as non-patterns. This is achieved by replacing the minimum ratio threshold s_r by a parameter k , which models the ratio of eligible triples at each level which are considered to be important. More formally, let \mathcal{T}_ℓ be the set of triples at level ℓ , which are minimal generalization of patterns at level $\ell - 1$. The patterns \mathcal{P}_ℓ at level ℓ are the k triples in \mathcal{T}_ℓ having the largest number of atomic patterns.

Definition 10 (ODT pattern (rank-based)) An ODT triple P at level ℓ is a rank-based ODT pattern if:

- there exists a minimal specialization of P which is a rank-based ODT pattern
- there are no more than k minimal generalizations of level- $(\ell - 1)$ rank-based ODT patterns that include more frequent atomic patterns than P .

5.3.1 Baseline approach for rank-based pattern enumeration

A baseline approach for enumerating rank-based patterns is to generate all eligible triples at each level ℓ , which are minimal generalizations of patterns at level $\ell - 1$. For each such triple, count its support (i.e., number of atomic patterns included in it). We may use the optimizations proposed in Section 4.2, to reduce the cost of generating ODT triples that are candidate patterns and counting their supports. After generating all triples and counting their supports, we select the top- k ones as patterns. Only these patterns are used to generate the candidate patterns at level $\ell + 1$.

5.3.2 Optimized rank-based pattern enumeration

To minimize the number of generated triples at each level ℓ and the effort for counting them, we examine the patterns at $\ell - 1$ in decreasing order of their potential to generate triples that will end up in the top- k triples at level ℓ . Hence, we access the patterns P at level $\ell - 1$ in decreasing order of their support $P.\text{cnt}$. For each such pattern P and for each minimal generalization $\text{Cand}P$ of P , we first compute the potential of $P' = \text{Cand}P - P$ to add to the support $\text{Cand}P.\text{cnt}$ (initially $\text{Cand}P.\text{cnt} = P.\text{cnt}$). If, by adding the maximum possible $P'.\text{cnt}$ to $\text{Cand}P.\text{cnt}$, $\text{Cand}P.\text{cnt}$ cannot make it to the top- k ℓ -triples so far, then we prune $\text{Cand}P$ and avoid its counting. The maximum possible $P'.\text{cnt}$ can be computed based on the following lemma:

Lemma 1. *The maximum possible $P'.\text{cnt}$ that can be added to $P.\text{cnt}$, to derive the support of $\text{Cand}P$ is as follows:*

- If $\text{Cand}P$ is generated by minimally generalizing $P.O$, then $P'.\text{cnt}$ equals $|P.D| \cdot |P.T|$.
- If $\text{Cand}P$ is generated by minimally generalizing $P.D$, then $P'.\text{cnt}$ equals $|P.O| \cdot |P.T|$.
- If $\text{Cand}P$ is generated by minimally generalizing $P.T$, then $P'.\text{cnt}$ equals $|P.O| \cdot |P.D|$.

Let θ be the k -th largest support of the triples generated so far at level ℓ . If for the next examined P from level $\ell - 1$ to generalize, P cannot be generalized to a $\text{Cand}P$ that may end up in the top- k level- ℓ triples, then we can immediately prune P . The condition for pruning P follows:

Lemma 2. *If $P.\text{cnt} + \max\{|P.D| \cdot |P.T|, |P.O| \cdot |P.O|, |P.O| \cdot |P.D|\} \leq \theta$, then no minimal generalization of P can enter the set of top- k level- ℓ ODT triples.*

Based on the above lemmas, we can prove the correctness of our enumeration algorithm for rank-based ODT patterns, described by Algorithm 2. The algorithm computes first all level-3 patterns \mathcal{P}_3 , based on the atomic pattern support threshold s_a (Lines 3–5). Having the patterns at level ℓ , the algorithm organizes those at level $\ell + 1$ in a priority queue (minheap) $\mathcal{P}_{\ell+1}$ of maximum size k . We consider all patterns P at level ℓ in decreasing order of support $P.\text{cnt}$, to maximize the potential of generating

Algorithm 2 Optimized Algorithm for enumerating rank-based ODT patterns

Require: a region graph $G(V, E)$; a trips table; a minimum support s_a for atomic ODT patterns; number k of top patterns to be generated at each level; maximum level considered ($maxl$)

```
1:  $\mathcal{T}_3$  = atomic triples computed from trips table
2:  $\mathcal{P}_3$  = triples in  $\mathcal{T}_3$  with support  $\geq s_a$ 
3: for all atomic triples  $P \in \mathcal{T}_3$  do
4:    $P.cnt = 1$  if  $P \in \mathcal{P}_3$ , else  $P.cnt=0$ 
5: end for
6:  $\ell = 3$ 
7: while  $|\mathcal{P}_\ell| > 0$  and  $\ell < maxl$  do ▷ extend level- $\ell$  patterns
8:    $\mathcal{P}_{\ell+1} = \emptyset$  ▷ Initialize  $k$ -minheap with level- $(\ell + 1)$  patterns
9:   for each  $P$  in  $\mathcal{P}_\ell$  in decreasing order of  $P.cnt$  do
10:    if  $|\mathcal{P}_{\ell+1}| = k$  and  $P.cnt + \max\{|P.D| \cdot |P.T|, |P.O| \cdot |P.O|, |P.O| \cdot |P.D|\} \leq$   

 $\mathcal{P}_{\ell+1}.top.cnt$  then
11:      continue ▷ Prune  $P$  based on Lemma 2
12:    end if
13:    if  $|\mathcal{P}_{\ell+1}| = k$  and  $P.cnt + |P.D| \cdot |P.T| \leq \mathcal{P}_{\ell+1}.top.cnt$  then
14:      for each minimal generalization  $CandP$  of  $P$  by origin do
15:        if  $CandP$  not considered before then
16:           $P' = CandP - P$ 
17:           $CandP.cnt = P.cnt + P'.cnt$ 
18:          if  $|\mathcal{P}_{\ell+1}| < k$  then
19:            add  $CandP$  to  $\mathcal{P}_{\ell+1}$ 
20:          else
21:            if  $CandP.cnt > \mathcal{P}_{\ell+1}.top.cnt$  then
22:              update  $\mathcal{P}_{\ell+1}$  with  $CandP$ 
23:            end if
24:          end if
25:        end if
26:      end for
27:    end if
28:    if  $|\mathcal{P}_{\ell+1}| = k$  and  $P.cnt + |P.O| \cdot |P.T| \leq \mathcal{P}_{\ell+1}.top.cnt$  then
29:      for each minimal generalization  $CandP$  of  $P$  by dest. do
30:        Lines 15 to 25 above
31:      end for
32:    end if
33:    if  $|\mathcal{P}_{\ell+1}| = k$  and  $P.cnt + |P.O| \cdot |P.D| \leq \mathcal{P}_{\ell+1}.top.cnt$  then
34:      for each minimal generalization  $CandP$  of  $P$  by time do
35:        Lines 15 to 25 above
36:      end for
37:    end if
38:  end for
39:   $\ell = \ell + 1$ 
40: end while
```

level- $(\ell + 1)$ triples of high support early. For each such pattern P , we first check if P can generate any level- $(\ell + 1)$ triple that can enter the set $\mathcal{P}_{\ell+1}$ of top- k triples so far at level $\ell + 1$, based on Lemma 2. If this is not possible, then P is pruned. Otherwise, we attempt to generalize P , first by adding an atomic region to $P.O$. If the maximum addition to $P.cnt$ by such an extension cannot result in a $CandP$ that can enter the top- k at level $\ell + 1$ (based on Lemma 1), then we do not attempt such extensions; otherwise we try all such extensions and measure their supports (Lines 15 to 25). We repeat the same for the possible extensions of $P.D$ and $P.T$. After $\mathcal{P}_{\ell+1}$ has been finalized, we use it to generate the top- k patterns at the next level. Since the number

of levels for which we can generate patterns can be very large, Algorithm 2 takes as a parameter the maximum level $maxl$ for which we are interested in generating patterns.

6 Approximate Computation and Sampling of ODT patterns

Due to the bottom-up, Apriori-style generation of candidates, the enumeration of large ODT patterns can be expensive. The combinations of atomic patterns that can formulate generalized ones exponentially increase as the generalized origins, destinations, and timeslots increase in size. The techniques described in the previous section reduce the cost of pattern enumeration by placing constraints or by ranking the ODT triples at each level and considering only the ones of highest support as patterns; hence, limiting the number of candidates at each level. Rank-based ODT patterns are essentially an approximate solution, which, however, does not avoid the potentially expensive level-wise pattern generation while risking missing some important patterns.

In this section, we investigate an alternative approximate solution to the pattern enumeration problem, which does not apply level-wise generation of candidate ODT patterns. Our proposal is a randomized solution, which targets the detection of ODT patterns of a certain size. Specifically, given a target size S_O of generalized origins O , a target size S_D of D , and a target size S_T of T , our approach efficiently generates-and-tests random ODT triples and keeps the ones that satisfy the support threshold s_r . Specifically, to generate a random candidate ODT pattern, our algorithm picks a random node $v \in V$ as seed and performs BFS around v to generate a connected subgraph with S_O nodes. This process is repeated $|V|$ times to generate $|V|$ subgraphs which form a set of O-candidates \mathcal{S}_O . We repeat the same to generate the D-candidates \mathcal{S}_D . Then, we pick random pairs of O- and D-candidates and complete them with random periods of S_T consecutive timeslots, to generate candidate ODT patterns. For each such candidate ODT-pattern, we count its support and add it to the set of approximate patterns if the support is greater than s_r .

6.1 Description and analysis

Figure 5 illustrates the process and Algorithm 3 presents its steps in detail. We first initialize the two sets \mathcal{S}_O and \mathcal{S}_D with the O-candidates and D-candidates, respectively. For each node $v \in V$, we place v in a new set S and perform a *random* BFS around v to form a random connected subgraph centered at v having exactly S_O nodes. To achieve this, we initialize a FIFO queue Q with the neighbors of v in the region neighborhood graph, in random order. At each step of the while loop (Lines 5–10), we dequeue the next node u from Q and if it is not part of S we add it u to S and its neighbors to Q in random order. As soon as S has S_O nodes, we terminate and add S to the set \mathcal{S}_O of the O-candidates. The nodes in S are guaranteed to form a connected subgraph, due to the BFS. Randomness in adding the neighbors guarantees that S is formed by a random subtree sized S_O , rooted at v , since there could be multiple such subtrees. The same BFS process is repeated to form a D-candidate from v to be added to \mathcal{S}_D (Lines 12–20). The time required to generate \mathcal{S}_O and \mathcal{S}_D is $O(|V|S_O)$ and $O(|V|S_D)$, respectively. Next, we collect into set \mathcal{T} all T-candidates as all subsequences of \mathcal{S}_O

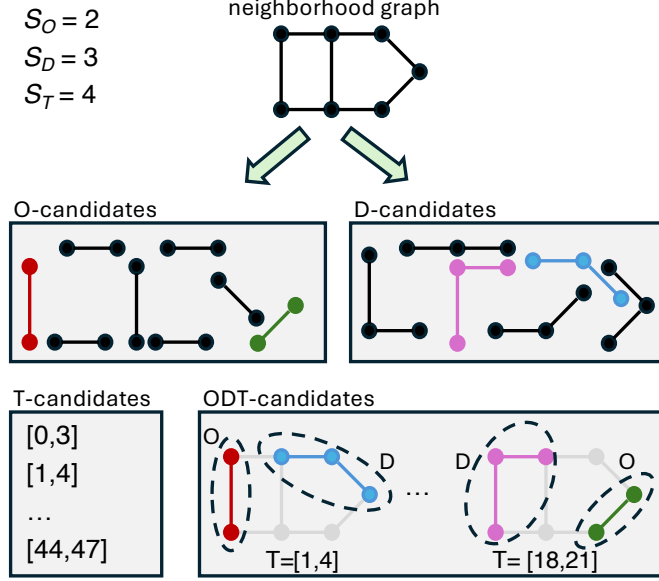


Fig. 5: Illustration of the approximate algorithm. Suppose that we are looking for patterns with 2 regions in the origin ($S_O = 2$), 3 regions in the destination ($S_D = 3$), and 4 timeslot ($S_T = 4$). We apply BFS from each node in the region neighborhood graph to generate candidate O and D components of the desired sizes and randomly pick them and combine them with random T periods of 4 timeslots to generate candidate ODT triples, which are eventually verified.

consecutive atomic timeslots, costing $O(|\mathcal{T}|)$ time, where $|\mathcal{T}|$ is the number of atomic timeslots. Finally (Lines 27–41), the algorithm picks M combinations of (O-candidate, D-candidate, T-candidate) triples (O, D, T) having $O \cap D \neq \emptyset$ (as per the requirement of ODT patterns), and counts their supports given the known set of atomic patterns. Recall that atomic patterns are the top s_a fraction of atomic triples by support, computed initially (at Line 1). If the ratio $cnt / (|O| \times |D| \times |\mathcal{T}|)$ is at least s_r , then (O, D, T) is added to the set of discovered patterns (Lines 60-62). The algorithm terminates after M sampling iterations and returns all discovered patterns.

Each randomly generated candidate ODT pattern includes $S_O \cdot S_D \cdot S_T$ atomic triples, hence counting the supports of M candidate ODT patterns to form the final set of results (Patterns) costs $O(M \cdot S_O \cdot S_D \cdot S_T)$. The space requirements of the algorithm are minimal, as we only generate one O-candidate and one D-candidate per graph node. In addition, we only generate at most one T-candidate per atomic timeslot. Hence, the space complexity is $O((S_O + S_D) \cdot |V| + |\mathcal{T}|)$.

6.2 A weighted approximate ODT pattern detection variant

Our approximate algorithm samples ODT candidates with equal probability. An improved version would pick ODT candidates that have higher probability to be ODT

Algorithm 3 Approximate Algorithm for ODT Pattern Discovery

Require: Graph $G(V, E)$, trips data, $s_a, s_r, S_O, S_D, S_T, M$

```
1: Compute atomic patterns (top  $s_a$  fraction by support)
   ▷ Step 1: Generate O and D candidates
2:  $S_O \leftarrow \emptyset, S_D \leftarrow \emptyset$ ; Patterns  $\leftarrow \emptyset$ 
3: for each node  $v \in V$  do
4:    $S \leftarrow \{v\}$ ; Initialize FIFO queue  $Q$  with neighbors of  $v$ , pushed to  $Q$  in random order
5:   while  $Q \neq \emptyset$  and  $|S| < S_O$  do
6:      $u \leftarrow \text{dequeue}(Q)$ 
7:     if  $u \notin S$  then
8:        $S \leftarrow S \cup \{u\}$ ; Push neighbors of  $u$  to  $Q$  in random order
9:     end if
10:  end while
11:  Add  $S$  to  $S_O$ 
   ▷ new O-candidate
12:   $S \leftarrow \{v\}$ 
13:  Initialize FIFO queue  $Q$  with neighbors of  $v$ , pushed to  $Q$  in random order
14:  while  $Q \neq \emptyset$  and  $|S| < S_D$  do
15:     $u \leftarrow \text{dequeue}(Q)$ 
16:    if  $u \notin S$  then
17:       $S \leftarrow S \cup \{u\}$ ; Push neighbors of  $u$  to  $Q$  in random order
18:    end if
19:  end while
20:  Add  $S$  to  $S_D$ 
   ▷ new D-candidate
21: end for
   ▷ Step 2: Generate  $T$  candidates
22:  $S_T \leftarrow \emptyset$ 
23: Let  $|\mathcal{T}|$  be the total number of timeslots
24: for each integer  $i \in [0, |\mathcal{T}| - S_T]$  do
25:   Add timeslot interval  $[i, i + S_T - 1]$  to  $S_T$ 
26: end for
   ▷ Step 3: Random sampling for ODT patterns
   ▷ Sample  $M$  random combinations
27: for  $i = 1$  to  $M$  do
28:   Pick random  $O \in S_O, D \in S_D, T \in S_T$ 
29:   if  $O \cap D \neq \emptyset$  then
30:      $i \leftarrow i - 1$ ; continue
   ▷ Repeat picking
31:   end if
32:   cnt  $\leftarrow 0$ 
33:   for each  $(o, d, t) \in O \times D \times T$  do
34:     if  $(o, d, t)$  is an atomic pattern then
35:       cnt  $\leftarrow \text{cnt} + 1$ 
36:     end if
37:   end for
38:   if  $\text{cnt} / (|O| \times |D| \times |T|) \geq s_r$  then
39:     Add  $(O, D, T)$  to Patterns
40:   end if
41: end for
42: return Patterns
```

patterns. For this, the O- D-, and T-candidates in S_O, S_D and S_T , respectively, are *weighted* and the M ODT pattern candidates are selected considering these weights. For the weighting, we use the following definitions:

1. For each node $v \in V$, we define as weight $w_O(v)$ the total number of atomic ODT patterns which include v as origin; we define as $w_D(v)$ the total number of atomic ODT patterns which include v as destination.

2. For each atomic timeslot $t \in \mathcal{T}$, we define as weight $w_T(t)$ the total number of atomic ODT patterns which include t .
3. For each set of nodes $S \subseteq V$, we define as weight $w_O(S)$ the sum $\sum_{v \in S} w_O(v)$ and as $w_D(S)$ the sum $\sum_{v \in S} w_D(v)$. Hence, each set S of nodes, which is an O-candidate in \mathcal{S}_O or a D-candidate in \mathcal{S}_D has a weight.
4. For each sequence T of consecutive atomic timestamps in \mathcal{T} which is a T-candidate, we define as weight $w_T(T)$ the sum $\sum_{t \in T} w_T(t)$.

Intuitively, combinations of O-, D-, and T-candidates with larger combined weight have higher probability to be an ODT pattern. Hence, we apply weighted ranking of the ODT candidates and use the top M candidates instead of uniformly sampling at random from the pool of ODT candidates. Algorithm 4 describes this weighted approximate ODT pattern detection method. First, we compute the $w_O(v)$ and $w_D(v)$ weights for each node v in the region neighborhood graph V . Then, we run Lines 3–21 of Algorithm 3 to compute the O-candidates and D-candidates as well as their respective w_O and w_D weights. The next step is to compute the weights of atomic timeslots and the T-candidates and their w_T weights. Finally, we enumerate all ODT candidates (combinations) and for each one we set its combined weight as the product of the weights of its O-, D-, and T- components (Line 13). While doing so, we update in a min-heap the top- M ODT candidates based on combined weights. In Lines 17–28, the supports of all these ODT candidates are computed and the ones which are ODT patterns are added to the Patterns result set.

Complexity Analysis Algorithm 4 initially scans once the set \mathcal{P}_3 of atomic patterns to generate the weights of the atomic regions (i.e., graph nodes) and the weights of the atomic timeslots. This costs $O(|\mathcal{P}_3|)$ time. Then, the O-candidates, D-candidates, and T-candidates are determined in $O(|V|S_O + |V|S_D + |\mathcal{T}|)$ time, as already discussed for Algorithm 3. Then, the algorithm enumerates all ODT candidates for the determination of the top- M candidates to be verified. This costs $O(S_O \cdot S_D \cdot S_T \cdot \log M)$ with the help of the priority queue (heap) H . Finally, the verification of the candidates costs $O(|\mathcal{P}_3| \cdot M)$. Overall, the total cost is $O(S_O \cdot S_D \cdot S_T \cdot \log M + |\mathcal{P}_3| \cdot M)$; if M is large compared to the number of ODT candidates, the $|\mathcal{P}_3| \cdot M$ factor dominates. The space complexity is just $O(|\mathcal{P}_3| + M)$ as we only need to store the atomic ODT patterns and the set of top- M ODT candidates to be verified.

7 Experimental Evaluation

In this section, we evaluate the performance of our proposed algorithms on real datasets. All methods were implemented in Python 3.14 and the experiments were run on a Macbook Pro with a M4 processor and 16GB memory. The source code of the paper is publicly available⁵.

⁵<https://github.com/kosyfakicse/Multi-granularity-ODT-patterns-Enumeration>

Algorithm 4 Weighed Approximate Algorithm for ODT Pattern Discovery

Require: Graph $G(V, E)$, trips data, $s_a, s_r, S_O, S_D, S_T, M$

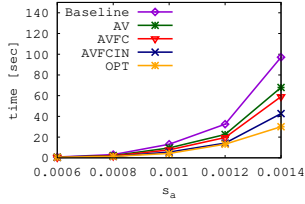
```
1: Compute atomic patterns (top  $s_a$  fraction by support)
2: For each node  $v \in V$ , use the atomic patterns to compute  $w_O(v)$  and  $w_D(v)$ 
    $\triangleright$  Step 1: Generate O and D candidates
3:  $S_O \leftarrow \emptyset, S_D \leftarrow \emptyset$ ; Patterns  $\leftarrow \emptyset$ 
4: Same as Lines 3–21 of Algorithm 3
5: For each O-candidate  $S \in S_O$  compute  $w_O(S)$ 
6: For each D-candidate  $S \in S_D$  compute  $w_D(S)$ 
7: For each node  $t \in T$ , use the atomic patterns to define  $w_T(t)$ 
    $\triangleright$  Step 2: Generate  $T$  candidates
8: Same as Lines 22–26 of Algorithm 3
9: For each T-candidate  $S \in S_T$  compute  $w_T(T)$ 
    $\triangleright$  Step 3: Examine ODT candidates in decreasing order of combined weight
10:  $H \leftarrow$  empty min-heap, to hold top- $M$  ODT candidates by combined weight
11: for all  $ODT, O \in S_O, D \in S_D, T \in S_T$  do
12:   if  $O \cap D = \emptyset$  then
13:      $w(ODT) \leftarrow w_O(O) \cdot w_D(D) \cdot w_T(T)$ 
14:     Update  $H$  to hold top- $M$  ODTs by  $w(ODT)$ 
15:   end if
16: end for
17: for  $i = 1$  to  $M$  do  $\triangleright$  For each ODT candidate in  $H$ 
18:    $ODT \leftarrow H[i]$ 
19:    $\text{cnt} \leftarrow 0$ 
20:   for each  $(o, d, t) \in O \times D \times T$  do
21:     if  $(o, d, t)$  is an atomic pattern then
22:        $\text{cnt} \leftarrow \text{cnt} + 1$ 
23:     end if
24:   end for
25:   if  $\text{cnt} / (|O| \times |D| \times |T|) \geq s_r$  then
26:     Add  $(O, D, T)$  to Patterns
27:   end if
28: end for
29: return Patterns
```

7.1 Dataset Description

For our experiments, we used three real datasets; NYC taxi trips, MTR network trips and Flights. Below, we provide a detailed description for each of them.

NYC taxi trips: We processed 7.5M trips of yellow taxis in NYC in January 2019, downloaded from TLC⁶. Each record represents a taxi trip and includes the pick-up and drop-off taxi zones (different regions in NYC), the date/time of the pick-up, and the number of passengers who took the trip. The 315 taxi zones represent atomic regions. We converted all time moments to 48 time-of-day slots (one slot per 30min intervals in the 24h). Then, we aggregated the data by merging all trips having the same origin, destination, and timeslot, and summing up the total number of passengers in all these trips to a total passenger flow, as explained in Section 3. This way, we ended up having 373460 unique ODT combinations (atomic ODT triples), which we used as input to our pattern enumeration algorithms. In addition, we used the maps posted at the same website to construct the neighboring graph G between the atomic regions (taxi zones). In G , we connected all pairs of atomic regions that share boundary points or are separated by water boundaries.

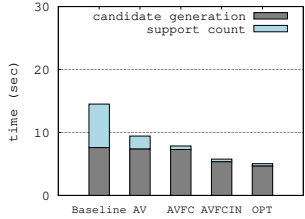
⁶<https://www.nyc.gov/site/tlc/about/tlc-trip-record-data.page>



(a) Taxi Network

(b) MTR Network

(c) Flights Network

Fig. 6: Pattern enumeration runtime, $s_r = 0.5$, varying s_a 

(a) Taxi Network

(b) MTR Network

(c) Flights Network

Fig. 7: Pattern enumeration cost breakdown, $s_r = 0.5$, default s_a

MTR trips: The Mass Transit Railway (MTR)⁷ is the biggest and the most popular public transport network operating in Hong Kong. The system consists of 168 stations, serving the areas of Hong Kong island, Kowloon and New Territories. We consider each station as an atomic region; we created the neighborhood graph G for them by linking stations that are next to each other in the network. MTR Corp. provided us with aggregate data for all passenger trips taken in September 2019. Specifically, for each atomic ODT triple, where the origin and destination are MTR stations and T is one of the 48 atomic timeslots, we have the total number of passenger trips in Sep. 2019. The total number of atomic ODT triples is 253497.

Flights: We extracted information for 5.8M US flights in 2015 from Kaggle⁸. In this dataset, we consider as atomic regions 319 airports in North America that appear in the file. Since the number of passengers in each flight was not given in the original data, we randomly generated a number between 50 and 200. We followed the same procedure as in for the two previous datasets; namely, we converted the original flights data into a table with atomic ODT triples. The total number of resulting ODT triples is 17623. To create the neighbor graph G , we follow the same logic as the two previous datasets; we connect atomic regions in neighboring states.

⁷<https://www.mtr.com.hk/en/customer/main/index.html>

⁸<https://www.kaggle.com/datasets/usdot/flight-delays?select=flights.csv>

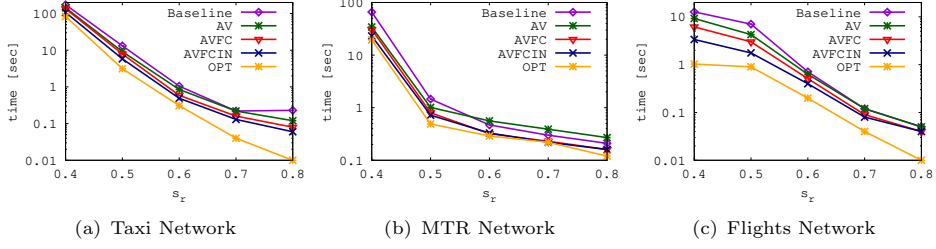


Fig. 8: Pattern enumeration runtime, default s_a , varying s_r .

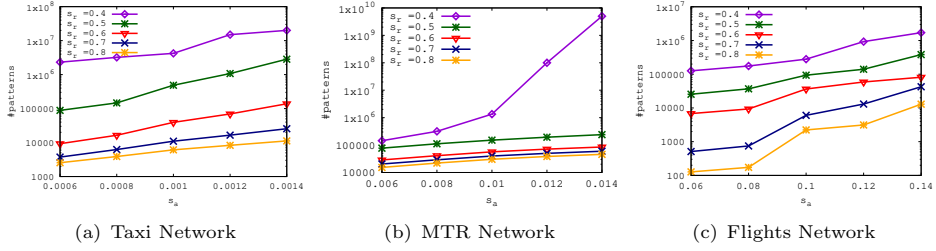


Fig. 9: Number of patterns for different values of s_a and s_r .

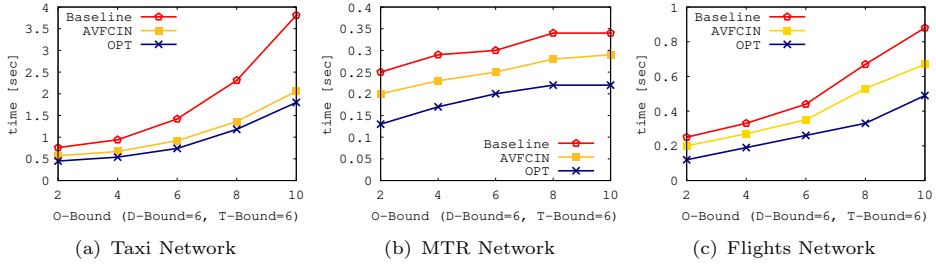


Fig. 10: Bounded pattern enumeration runtime, default s_a , s_r , varying origin bound

7.2 Pattern enumeration

We start by evaluating the performance of our baseline pattern enumeration algorithm, described in Section 4.1, and its optimizations, described in Section 4.2. Specifically, we compare the performance of the following methods:

- Algorithm 1, denoted by Baseline.
- Algorithm 1 with the avoid recounting P' optimization, denoted by AV.
- Algorithm 1 with the avoid recounting P' and fast check for zero support of P' optimizations, denoted by AVFC.

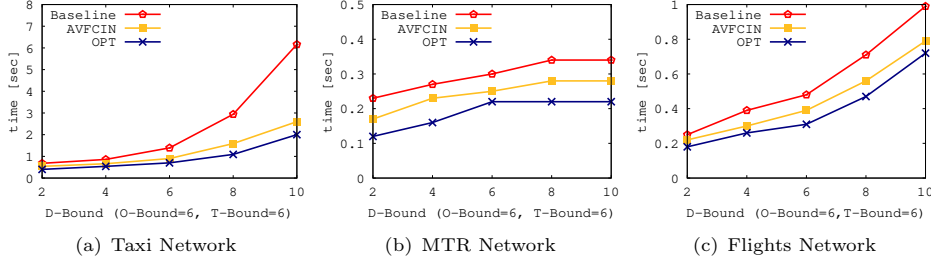


Fig. 11: Bounded pattern enumeration runtime, default s_a , s_r , varying destination bound

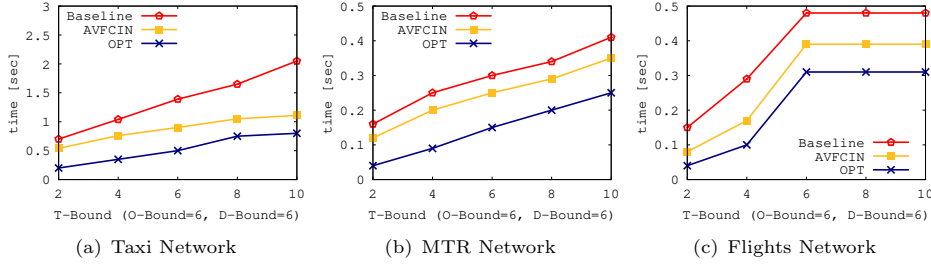


Fig. 12: Bounded pattern enumeration runtime, default s_a , s_r , varying timeslot bound

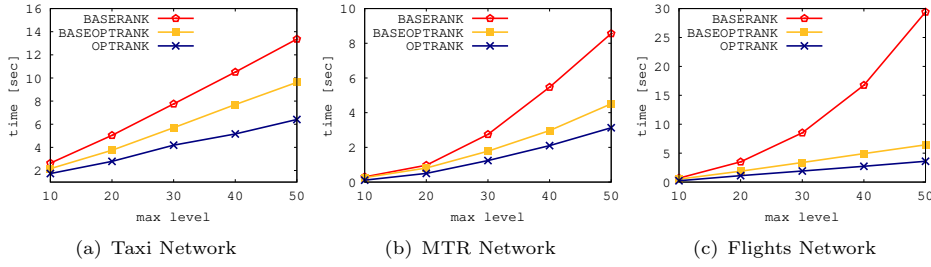


Fig. 13: Rank-based pattern enumeration, $s_a = 0.1$, $k = 3000$, varying $maxl$

- Algorithm 1 with the avoid recounting P' , fast check, and improved neighborhood optimizations, denoted by AVFCIN.
- Algorithm 1 with all four optimizations, denoted by OPT.

Figure 6 shows the costs of all tested methods on the three datasets for various values of s_a (default $s_a = 0.001$ for Taxi, $s_a = 0.01$ for MTR and Flights), while keeping s_r fixed to 0.5. Observe that the optimizations pay off, since the initial cost of the baseline approach drops to about 50% of the initial cost. When comparing between the different optimizations, we observe that the ones that have the biggest impact are

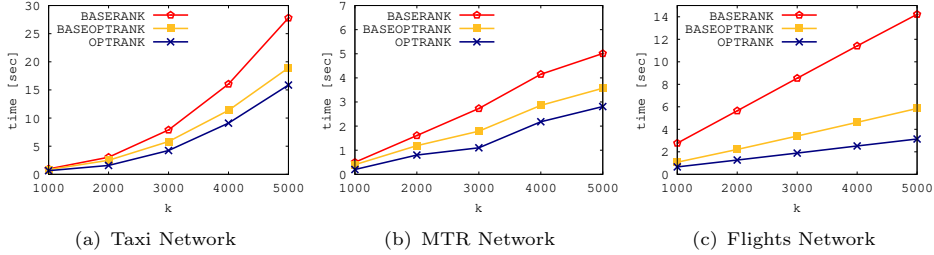


Fig. 14: Rank-based pattern enumeration, $s_a = 0.1$, $maxl = 30$, varying k

the P' counting avoidance and the improved neighborhood computation. The savings by the prefix sum optimization are not impressive, because the other optimizations already reduce a lot the number of candidates for which exact counting is required.

This assertion is confirmed by the cost-breakdown experiment shown in Figure 7, where for the default values of s_a and s_r , we show the fraction of the cost that goes to candidate pattern generation and support counting. Note that the baseline approach spends most of the time in pattern counting, as the candidate generation process is quite simple. On the other hand, the optimized versions of the algorithm trade off time for pattern generation (spent on bookkeeping all generated triples at each level, bookkeeping OD pairs with at least one trip, etc.) to reduce the time spent on support counting. Note that the ratio of the time spent on support counting is eventually minimized. When comparing between the different versions, we observe that the candidate generation time drops as more optimizations are employed (e.g., fast check for zero support). Since finding all patterns at level ℓ requires considering all possible extensions of patterns at level $\ell - 1$, we note that there is little room for further reducing the cost of ODT pattern enumeration; in this respect OPT is the best approach that one can apply if the goal is to find all ODT patterns.

Figure 8 shows the runtime cost of pattern enumeration for different values of s_r , by keeping s_a to its default value. Observe that the cost explodes for values of s_r smaller than 0.5. The reason is that small s_r values make it easy for triples at each level to be characterized as patterns, which, in turn, greatly increases the number of candidates and patterns at the next level. On the other hand, for $s_r \geq 0.5$ at least half of the atomic triples in a candidate must be atomic patterns, which restricts the number of candidates and patterns at all levels.

The next experiment proves the pattern explosion for small values of s_r . The high cost of pattern enumeration stems from the fact that a very large number of patterns are found at each level, which, in turn, all have to be minimally generalized due to the weak monotonicity property of Definition 9. Figure 9 shows the numbers of enumerated patterns for different values of s_a and s_r . As the number of patterns grow, so does the essential cost of candidate generation, which becomes the dominant cost factor. From Figure 9, we observe that the number of enumerated patterns is very sensitive to s_r . Specifically, for values of s_r smaller than 0.5 the number of patterns explode. On the other hand, the sensitivity to s_a is relatively low. Still, even for the default values of s_a (0.001 for Taxi and 0.01 for MTR and Flights) there are thousands or even millions of

qualifying patterns. Such huge numbers necessitate the use of constraints or ranking in order to limit the number of patterns, focusing on the most important ones.

Memory Requirements Table 3 shows the runtime performance (sec), the number of patterns, and the memory requirements (GB) of all methods for different values of s_a on the Taxi dataset. Observe that the baseline algorithm requires significantly less memory compared to the optimized methods, as it does not bookkeep any information (counted triples at each level, $r.dests$ and $r.srcs$ for each atomic region r , prefix-sums, etc.) Still, the additional memory requirements by the optimized methods are bearable and come with significant cost savings, as we have discussed already. In addition, large s_a values that have increased memory requirements result in a huge number of patterns, which may not be informative.

Table 3: Peak memory used varying s_a , default s_r - Taxi Network

| s_a | Performance | Baseline | AV | AVFC | AVFCIN | OPT |
|--------|-------------|----------|-------|-------|--------|-------|
| 0.001 | #patterns | 485K | 485K | 485K | 485K | 485K |
| | Memory (GB) | 0.38 | 0.83 | 0.95 | 0.97 | 0.99 |
| | Time (sec) | 13.1 | 9.5 | 7.6 | 5.5 | 4.9 |
| 0.0012 | #patterns | 1.07M | 1.07M | 1.07M | 1.07M | 1.07M |
| | Memory (GB) | 0.79 | 1.42 | 1.61 | 1.92 | 2.1 |
| | Time (sec) | 32.46 | 22.52 | 19.5 | 14 | 13.2 |
| 0.0014 | #patterns | 2.8M | 2.8M | 2.8M | 2.8M | 2.8M |
| | Memory (GB) | 1.1 | 2.72 | 2.88 | 2.99 | 3.4 |
| | Time (sec) | 97.7 | 67.9 | 59.8 | 42.7 | 30.3 |
| 0.0016 | #patterns | 23.6M | 23.6M | 23.6M | 23.6M | 23.6M |
| | Memory (GB) | 5.6 | 7.02 | 7.28 | 7.69 | 8.04 |
| | Time (sec) | 529.4 | 288.9 | 261.1 | 242.6 | 229.8 |

7.3 Bounded patterns

As discussed in Section 5.1, one way to limit the number of patterns is to bound the number of atomic regions and/or atomic timeslots in them. In the next experiment, we study the effect of such pattern size constraints to the runtime of algorithms Baseline, AVFCIN, and OPT. We run experiments by setting s_a and s_r to their default values. In each experiment, we set a fixed upper bound to the sizes of two of O, D, and T, and vary the bound of one. Hence, in Figure 10, we keep the upper size bounds of D and T fixed and we vary the upper size bound of O; in Figure 11, we keep the upper size bounds of O and T fixed and we vary the upper size bound of D; in Figure 12, we keep the upper size bounds of O and D fixed and we vary the upper size bound of T. In general, the cost increases as one bound increases, which is as expected, because the number of patterns and generated candidates increases as well. On certain datasets (e.g., MTR), the cost growth is slow when the bound of O or D is increased; this is due to the fact that the number of patterns at low levels is already quite small and the generated patterns start to decrease as we change levels, so the bound increase does not affect the cost significantly. On the other hand, when the bound of T increases (Figure 12), there is a stable increase of time in all datasets. This is due to the fact that the number of atomic timeslots is significantly small and neighboring timeslots

are highly correlated in terms of flow. When comparing the costs of Baseline, AVFCIN, and OPT, we observe that OPT maintains a significant performance advantage for different bound values, especially on MTR.

7.4 Rank-based patterns

We now evaluate the performance of rank-based pattern enumeration, described in Section 5.3. We compare three algorithms. The first one is the baseline approach described in Section 5.3.1, without the pattern enumeration optimizations described in Section 4.2. The second one is the baseline approach of Section 5.3.1 with the pattern enumeration optimizations described in Section 4.2. The third approach is the optimized algorithm for rank-based patterns described in Section 5.3.2. The three approaches are denoted by BASERANK, BASEOPTRANK, and OPTRANK, respectively.

Figure 13 shows the runtime cost of the three algorithms for $s_a = 0.1$ and $k = 3000$ patterns per level, as a function of the maximum level $maxl$ of patterns that we generate and enumerate. Recall that the top- k patterns selected per level may generate numerous triples at the next level and there is no s_r threshold to reduce them, so the number of levels can become too large. We use $maxl$ as a parameter for limiting the sizes of patterns. As shown in the figure, OPTRANK maintains a large advantage over the other approaches which do not take advantage of the pruning conditions and the ranking of generated triples. Figure 14 shows the runtime cost of the algorithms for $s_a = 0.1$ and various values of k , after setting $maxl = 30$. The advantage of OPTRANK over the other algorithms is not affected by k . Overall, despite the fact that a very high value of s_a is used, due to the fact that the number of patterns per level is limited by k , all algorithms are scalable, making pattern enumeration practical, even in cases where the number of possible ODT combinations is huge.

7.5 Approximate patterns

In this section, we evaluate the efficiency and effectiveness of our approximate algorithm for ODT patterns detection and its weighted variant, presented in Section 6. Once again, we used our three real datasets which present different characteristics with respect to the graph size and complexity and with respect to the atomic ODT patterns that they may have. For different datasets and problem parameter values, we compare three approaches: the most efficient version of the exact algorithm (AVFCIN optimization), the approximate algorithm (described in Section 6.1), and its weighted variant (described in Section 6.2). The approximate algorithms draw and verify $M = 1\text{mil}$ ODT candidates (either by sampling or after ranking).

7.5.1 Effect of Varying s_a

We first test the effect of the parameter s_a . For various values s_a , Table 4 shows the runtime and the number of detected patterns by the tested methods. In the experiment, we fixed the value of $s_r = 0.5$ and we are looking for ODT patterns, where O includes 4 regions, D includes 4 regions, and T includes 4 atomic timeslots, i.e., $S_O = S_D = S_T = 4$. In some experimental instances the exact algorithm took longer than 180 seconds

and it was terminated it before it could enumerate any patterns. In these experiments, we marked the runtime and the number of patterns of the exact algorithm by “—”.

Observe that the cost of the exact algorithm increases with s_a and the algorithm cannot produce any patterns within 3 minutes when s_a is higher than 0.02 on the Taxi dataset. This is due to the facts that (i) Taxi is a large dataset and the number of atomic patterns compared to other datasets becomes very large as s_a increases, and (ii) the Taxi network is quite dense (e.g., denser than the MTR network), so the number of candidate patterns at each level becomes high. The approximate algorithm shows stable performance across all tested s_a values, with runtimes between 3-6 seconds. This is expected, since the algorithm evaluates a fixed number $M = 1\text{mil}$ of candidate ODT patterns.

The weighted-approximate algorithm verifies fewer ODT candidates compared to the unweighted version (10k instead 1mil), so it completes faster. On Taxi with $s_a = 0.015$, the exact algorithm requires 4.57 seconds, while the weighted method completes in 1.00 second. On MTR, the cost increases from 0.13 seconds at $s_a = 0.015$ to 0.63 seconds at $s_a = 0.05$ for the exact algorithm. The weighted method maintains sub-second runtime across all configurations. In all cases, the weighted approximate algorithm runs much faster than the unweighted algorithm, while producing more patterns. On MTR and Flights a significant proportion of the exact result is detected by the approximate methods, however, their cost difference to the exact method is not high (the approximate methods may even be slower). On Taxi, the weighted approximate algorithm produces a representative sample of the patterns within a short time. The reason behind the fact that the weighted method is faster than the sampling approximate algorithm is that the weighted method focuses evaluation on high-probability candidates by ranking all possible ODT triples by their weight (based on the number of atomic patterns each node/timeslot participates in) and checking only the top $M=10\text{k}$ candidates. In contrast, the approximate method randomly samples $M=1\text{mil}$ candidates with equal probability. Since patterns are not uniformly distributed in the search space, the weighted approach evaluates fewer low-probability candidates and finds valid patterns more efficiently.

7.5.2 Effect of Varying s_r

Table 5 compares the methods for various values of s_r , having fixed s_a to 0.015 and $S_O = S_D = S_T = 4$. Reducing s_r increases the cost for the exact algorithm, as more ODT triples qualify as patterns when the support ratio requirement is relaxed. For the Taxi Network at $s_r = 0.3$, the exact algorithm requires 11.46 seconds to find all 271k patterns. Both approximate methods show stable performance across all s_r values, since they evaluate a fixed number of candidates.

The weighted method completes within under 1 second across all datasets and s_r values. On the MTR Network, the exact algorithm completes in under 1 second at all tested s_r values, with pattern counts ranging from 83 to 698. The exact method runs faster than the sampling approximate method because the sparsity of the network greatly limits the number of generated candidates at each level, hence, the total number of generated ODT candidates for $S_O = S_D = S_T = 4$ is relatively small. Overall, the weighted approximate algorithm is worth using in dense networks, where

Table 4: Performance and pattern count for varying s_a with default $s_r = 0.5$, $S_O = S_D = S_T = 4$

| Method | Taxi Network | | MTR Network | | Flight Network | |
|-----------------------------|--------------|-----------|-------------|-----------|----------------|-----------|
| | Time (sec) | #patterns | Time (sec) | #patterns | Time (sec) | #patterns |
| $s_a = 0.015$ | | | | | | |
| Exact | 4.57 | 62.1k | 0.13 | 83 | 0.16 | 4 |
| Approx. ($M=1\text{mil}$) | 3.08 | 24 | 2.97 | 24 | 2.92 | 1 |
| Weighted ($M=10\text{k}$) | 1.00 | 55 | 0.32 | 25 | 0.81 | 2 |
| $s_a = 0.02$ | | | | | | |
| Exact | 7.7 | 124k | 0.18 | 210 | 0.25 | 4 |
| Approx. ($M=1\text{mil}$) | 6.12 | 212 | 2.97 | 52 | 3.01 | 0 |
| Weighted ($M=10\text{k}$) | 1.00 | 627 | 0.33 | 53 | 0.80 | 2 |
| $s_a = 0.05$ | | | | | | |
| Exact | 38.1 | 715k | 0.63 | 2,056 | 1.20 | 60 |
| Approx. ($M=1\text{mil}$) | 3.14 | 1k | 3.08 | 788 | 3.05 | 15 |
| Weighted ($M=10\text{k}$) | 0.6 | 2.19k | 0.34 | 536 | 0.84 | 23 |

Table 5: Performance and pattern count for varying s_r with default $s_a = 0.015$, $S_O = S_D = S_T = 4$

| Method | Taxi Network | | MTR Network | | Flight Network | |
|-----------------------------|--------------|-----------|-------------|-----------|----------------|-----------|
| | Time (sec) | #patterns | Time (sec) | #patterns | Time (sec) | #patterns |
| $s_r = 0.3$ | | | | | | |
| Exact | 11.46 | 271k | 0.21 | 698 | 0.86 | 154 |
| Approx. ($M=1\text{mil}$) | 2.93 | 227 | 2.99 | 240 | 2.97 | 15 |
| Weighted ($M=10\text{k}$) | 0.92 | 509 | 0.32 | 206 | 0.77 | 23 |
| $s_r = 0.4$ | | | | | | |
| Exact | 5.24 | 145k | 0.14 | 329 | 0.30 | 4 |
| Approx. ($M=1\text{mil}$) | 0.45 | 77 | 3.14 | 112 | 2.83 | 1 |
| Weighted ($M=10\text{k}$) | 0.92 | 280 | 0.32 | 103 | 0.84 | 2 |
| $s_r = 0.5$ | | | | | | |
| Exact | 4.57 | 62.1k | 0.13 | 83 | 0.16 | 4 |
| Approx. ($M=1\text{mil}$) | 3.08 | 24 | 2.97 | 24 | 2.92 | 1 |
| Weighted ($M=10\text{k}$) | 1.00 | 55 | 0.32 | 25 | 0.81 | 2 |

it can detect a good proportion of patterns within a certain time bound, as opposed to the exact method, which operates level by level and takes longer time to generate and verify (more) ODT candidates.

7.5.3 Effect of Varying S_O, S_D, S_T

Table 6 reports runtime and pattern count for different values of the sizes (S_O, S_D, S_T) of the pattern components. In all experiments, we fixed $s_a = 0.015$ and $s_r = 0.5$.

As we increase the bounds from (3,3,3) to (4,4,4), we observe how the computational cost and pattern counts change. For the smaller configurations with $S_T = 3$, the exact algorithm shows stable performance on the Taxi Network, completing in 12.21 seconds at (3,3,3) and finding 271,444 patterns. As we increase the time dimension to $S_T = 4$ and $S_T = 5$ while keeping $S_O = S_D = 3$, the exact algorithm’s runtime increases from 12.21 seconds to 24.46 seconds on Taxi, while pattern counts remain at similar levels (271k to 300k). The approximate method scales from 3.16 seconds to 4.30 seconds across these configurations, discovering between 210 and 244 patterns. The weighted method maintains consistent sub-second performance, completing in around 1 second across all configurations from (3,3,3) to (3,3,5), while finding 2 to 3 times more patterns than the unweighted approximate method.

At the (4,4,4) configuration, the exact algorithm requires 4.57 seconds on the Taxi Network and finds 62.1k patterns. This shows a significant reduction in pattern count compared to the (3,3,3) configuration, which is expected as larger patterns impose stricter structural constraints. The approximate method requires 3.08 seconds and finds only 24 patterns, while the weighted method completes in 1.00 second and finds 55 patterns. On the MTR Network at (4,4,4), the exact algorithm completes in only 0.13 seconds finding 83 patterns, demonstrating the efficiency gains on sparser networks.

At the largest configuration (5,5,4), the exact algorithm times out on all three datasets. The approximate method requires 8-9 seconds, while the weighted method maintains around 1 second runtime. On the Taxi Network at (5,5,4), the approximate method finds 8,677 patterns while the weighted method finds 8,981 patterns, showing that at very large pattern sizes both methods discover substantial numbers of patterns. On the MTR Network at (5,5,4), the approximate method finds 6,812 patterns while the weighted method finds 1,870 patterns. On the Flight Network, pattern counts are low across all configurations.

Table 7 summarizes the runtime comparison across three representative configurations. The results show that the approximate methods are not worth applying when the pattern size parameters (S_O, S_D, S_T) are small or when the network is sparse (MTR). On the other hand on dense networks (Taxi) or for large pattern size parameters, the weighted approximate algorithm is consistently superior compared to the exact method in terms of runtime and it is worth applying. When comparing the two versions of the approximate algorithm, the weighted method prevails as it completes faster (typically 3-8 times), while finding a similar number of patterns compared to the unweighted approximate method.

Overall, the exact algorithm is limited by its high computational cost on dense networks like Taxi, particularly at large pattern sizes. The approximate methods provide stable, predictable performance. The choice of algorithm depends on completeness requirements: the exact algorithm guarantees finding all patterns when it can complete, while the approximate methods enable discovery of large patterns in cases where the exact method times out.

Table 6: Performance and pattern count for different combinations of O, D, T bounds with $s_a = 0.015$, $s_r = 0.5$

| Method | Taxi Network | | MTR Network | | Flight Network | |
|--|--------------|-----------|-------------|-----------|----------------|-----------|
| | Time (sec) | #patterns | Time (sec) | #patterns | Time (sec) | #patterns |
| <i>S_O=3, S_D=3, S_T=3</i> | | | | | | |
| Exact | 12.21 | 271k | 0.21 | 698 | 0.85 | 154 |
| Approx. (<i>M</i> =1mil) | 3.16 | 210 | 3.15 | 249 | 2.95 | 11 |
| Weighted (<i>N</i> =10K) | 1.02 | 509 | 0.33 | 206 | 0.81 | 23 |
| <i>S_O=3, S_D=3, S_T=4</i> | | | | | | |
| Exact | 17.69 | 300k | 0.28 | 733 | 1.08 | 44 |
| Approx. (<i>M</i> =1mil) | 3.77 | 244 | 3.58 | 271 | 3.37 | 1 |
| Weighted (<i>N</i> =10K) | 0.94 | 557 | 0.32 | 230 | 0.83 | 4 |
| <i>S_O=3, S_D=3, S_T=5</i> | | | | | | |
| Exact | 24.46 | 280k | 0.35 | 606 | 1.27 | 8 |
| Approx. (<i>M</i> =1mil) | 4.30 | 214 | 4.10 | 222 | 4.06 | 2 |
| Weighted (<i>N</i> =10K) | 0.94 | 518 | 0.33 | 201 | 0.81 | 4 |
| <i>S_O=4, S_D=4, S_T=4</i> | | | | | | |
| Exact | 4.57 | 62.1k | 0.13 | 83 | 0.16 | 4 |
| Approx. (<i>M</i> =1mil) | 3.08 | 24 | 2.97 | 24 | 2.92 | 1 |
| Weighted (<i>N</i> =10K) | 1.00 | 55 | 0.32 | 25 | 0.81 | 2 |
| <i>S_O=5, S_D=5, S_T=4</i> | | | | | | |
| Exact | — | — | — | — | — | — |
| Approx. (<i>M</i> =1mil) | 8.44 | 8,677 | 7.72 | 6.8k | 8.96 | 0 |
| Weighted (<i>N</i> =10K) | 1.14 | 8,981 | 0.38 | 1.8k | 0.81 | 0 |

Table 7: Runtime comparison (in seconds) for different O, D, T configurations with $s_a = 0.015$, $s_r = 0.5$

| Dataset | <i>S_O=3, S_D=3, S_T=3</i> | | | <i>S_O=4, S_D=4, S_T=4</i> | | | <i>S_O=5, S_D=5, S_T=4</i> | | |
|---------|--|---------|----------|--|---------|----------|--|---------|----------|
| | Exact | Approx. | Weighted | Exact | Approx. | Weighted | Exact | Approx. | Weighted |
| Taxi | 12.21 | 3.16 | 1.02 | 4.57 | 3.08 | 1.00 | timeout | 8.44 | 1.14 |
| MTR | 0.21 | 3.15 | 0.33 | 0.13 | 2.97 | 0.32 | timeout | 7.72 | 0.38 |
| Flight | 0.85 | 2.95 | 0.81 | 0.16 | 2.92 | 0.81 | timeout | 8.96 | 0.81 |

7.6 Use cases

Lastly, we explore the use of ODT patterns in real-world applications. To do that, we restricted the origin and time dimensions, according to Section 5.2, and identified the most popular destinations for different times of the day. In the first experiment, we used the Taxi dataset. Table 8 shows some of these patterns. We first restricted O to be Financial District, Manhattan and T to morning, lunch, and afternoon timeslots. This gave us the most popular destinations during these timeslots, extended region Greenwich Village South and North, and Tribeca, extended region Greenwich Village

South and North, Tribeca and Battery Park, and extended region MidTownEast and Centre, Murray Hill, Union Square, and Stuy Town. Our study shows that people tend to move toward residential areas or popular dining spots like Union Square during the afternoon, suggesting a preference for destinations near their homes by the end of the day. An interesting observation is the shift in movement across districts during lunch, possibly due to limited dining options in the Financial District. Insights like these could help restaurant owners identify ideal locations for new establishments, considering the demand in these areas.

Table 8: Use case - Taxi Dataset

| Origin | Timeslots | popular destinations |
|-------------------|---------------|--|
| FinancialDistrict | [8:30-9:30] | GreenwichVillageS, GreenwichVillageN |
| FinancialDistrict | [8:30-9:30] | GreenwichVillageS, GreenwichVillageN, Tribeca |
| FinancialDistrict | [12:30-14:00] | GreenwichVillageS, GreenwichVillageN, Tribeca |
| FinancialDistrict | [12:30-14:00] | GreenwichVillageS, GreenwichVillageN, Tribeca, BatteryPark |
| FinancialDistrict | [17:30-19:30] | MidTownCentre, MidTownEast, MurrayHill |
| FinancialDistrict | [17:30-19:30] | MidTownCentre, MidTownEast, MurrayHill, Union Square, StuyTown |

We repeated the experiment on the MTR data to obtain some interesting patterns, such as those shown in Table 9 considering different origin points. As representative patterns, we show popular destinations for people who move from popular regions such as Mong Kok in morning peak hours. The extracted patterns show that the most popular destinations are an extended region covering the center of Hong Kong (e.g., Central) and extended regions which includes the city center and destinations from the city center along the north coast of Hong Kong island. In case of an service disruption incident at the origin, the transportation company can use our approach to extract constrained patterns to predict the travel needs of affected passengers and schedule emergency transportation for them (e.g., buses).

Table 9: Use case - MTR Dataset

| Origin | Timeslots | popular destinations |
|----------|---------------|--|
| Mong Kok | [8:30-9:30] | [Central-Admiralty] |
| Mong Kok | [8:30-9:30] | [Central-Admiralty],[Exhibition Centre-University] |
| Wan Chai | [17:30-18:30] | [North Point-Quarry Bay] |
| Wan Chai | [17:30-18:30] | [North Point-Quarry Bay][Yau Tong-Kwun Tong] |

8 Conclusions

In this paper, we have studied the problem of enumeration origin-destination-timeslot (ODT) patterns at varying granularity from a database of trips. To our knowledge, this is the first work that formulates and studies this problem. Due to the huge number of region-time combinations that can formulate a candidate pattern, the problem is hard. We explore the problem space level-by-level, buiding on a weak monotonicity property

of patterns. We propose a number of optimizations that greatly reduce the cost of the baseline pattern enumeration algorithm. To eliminate the possibly huge number of ODT patterns, which take too long to enumerate and analyze, we propose practical variants of the mining problem, where we restrict the size of patterns and/or the regions/timeslots included in them. In addition, we suggest an interesting definition of rank-based patterns and we study their efficient enumeration. Finally, we propose an approximate algorithm and a weighted version of it, which can detect representative patterns of a given size much faster than the exact algorithm. Experiments with three real datasets demonstrate the effectiveness of the proposed techniques. In the future, we plan to study database queries that apply on the trips table, to analyze the outflow (or inflow) of generalized regions to (or from) other regions at specific time intervals. Such a tool, together with our pattern enumeration tools can assist transportation analysts or companies in planning or restructuring.

References

- [1] Kosyfaki, C., Mamoulis, N., Cheng, R., Kao, B.: Generalized origin-destination-time flow patterns. In: Proceedings of the 19th International Symposium on Spatial and Temporal Data, SSTD 2025, Osaka, Japan, August 25-27, 2025, pp. 159–170. ACM, ??? (2025)
- [2] Liu, J., Li, T., Ji, S., Xie, P., Du, S., Teng, F., Zhang, J.: Urban flow pattern mining based on multi-source heterogeneous data fusion and knowledge graph embedding. *IEEE Trans. Knowl. Data Eng.* **35**(2), 2133–2146 (2023)
- [3] Wang, Y., Yin, H., Chen, H., Wo, T., Xu, J., Zheng, K.: Origin-destination matrix prediction via graph convolution: a new perspective of passenger demand modeling. In: Proceedings of the 25th ACM SIGKDD International Conference on Knowledge Discovery & Data Mining, KDD, Anchorage, AK, USA, pp. 1227–1235 (2019)
- [4] Yu, Q., Gu, Y., Yang, S., Zhou, M.: Discovering spatiotemporal patterns and urban facilities determinants of cycling activities in beijing. *Journal of Geovisualization and Spatial Analysis* **5**(1), 16 (2021)
- [5] Du, B., Peng, H., Wang, S., Bhuiyan, M.Z.A., Wang, L., Gong, Q., Liu, L., Li, J.: Deep irregular convolutional residual LSTM for urban traffic passenger flows prediction. *IEEE Trans. Intell. Transp. Syst.* **21**(3), 972–985 (2020)
- [6] Fang, Z., Long, Q., Song, G., Xie, K.: Spatial-temporal graph ODE networks for traffic flow forecasting. In: KDD: The 27th ACM SIGKDD Conference on Knowledge Discovery and Data Mining, Virtual Event, Singapore, pp. 364–373 (2021)
- [7] Xie, P., Li, T., Liu, J., Du, S., Yang, X., Zhang, J.: Urban flow prediction from spatiotemporal data using machine learning: A survey. *Information Fusion* **59**,

- [8] Agrawal, R., Srikant, R.: Mining sequential patterns. In: Proceedings of the Eleventh International Conference on Data Engineering, IEEE Computer Society, Taipei, Taiwan, pp. 3–14 (1995)
- [9] Alvares, L.O., Bogorny, V., Kuijpers, B., Macêdo, J.A.F., Moelans, B., Vaisman, A.A.: A model for enriching trajectories with semantic geographical information. In: 15th ACM International Symposium on Geographic Information Systems, ACM-GIS, November 7–9, Seattle, Washington, USA, Proceedings, p. 22 (2007)
- [10] Cai, Y., Ng, R.T.: Indexing spatio-temporal trajectories with chebyshev polynomials. In: Proceedings of the ACM SIGMOD International Conference on Management of Data, Paris, France, pp. 599–610 (2004)
- [11] Fan, Q., Zhang, D., Wu, H., Tan, K.: A general and parallel platform for mining co-movement patterns over large-scale trajectories. *Proc. VLDB Endow.*, 313–324 (2016)
- [12] Giannotti, F., Nanni, M., Pinelli, F., Pedreschi, D.: Trajectory pattern mining. In: Proceedings of the 13th ACM SIGKDD International Conference on Knowledge Discovery and Data Mining, San Jose, California, USA, pp. 330–339 (2007)
- [13] Gudmundsson, J., Laube, P., Wolle, T.: Movement patterns in spatio-temporal data. In: *Encyclopedia of Springer GIS*, pp. 726–732 (2008)
- [14] Kalnis, P., Mamoulis, N., Bakiras, S.: On discovering moving clusters in spatio-temporal data. In: *Advances in Spatial and Temporal Databases, 9th International Symposium, SSTD, Angra Dos Reis, Brazil, Springer. Lecture Notes in Computer Science*, vol. 3633, pp. 364–381 (2005)
- [15] Beernaerts, J., Debever, E., Lenoir, M., Baets, B.D., Weghe, N.V.: A method based on the levenshtein distance metric for the comparison of multiple movement patterns described by matrix sequences of different length. *Expert Syst. Appl.* **115**, 373–385 (2019)
- [16] Behara, K.N.S., Bhaskar, A., Chung, E.: Geographical window based structural similarity index for origin-destination matrices comparison. *J. Intell. Transp. Syst.* **26**(1), 46–67 (2022)
- [17] Duan, Z., Zhang, K., Chen, Z., Liu, Z., Tang, L., Yang, Y., Ni, Y.: Prediction of city-scale dynamic taxi origin-destination flows using a hybrid deep neural network combined with travel time. *IEEE Access* **7**, 127816–127832 (2019)
- [18] Kumarage, S., Yildirimoglu, M., Zheng, Z.: A hybrid modelling framework for the estimation of dynamic origin–destination flows. *Transportation Research Part B: Methodological* **176** (2023)

- [19] Ros-Roca, X., Montero, L., Barceló, J., Nökel, K., Gentile, G.: A practical approach to assignment-free dynamic origin–destination matrix estimation problem. *Transportation Research Part C: Emerging Technologies* **134** (2022)
- [20] Jin, R., Liu, L., Ding, B., Wang, H.: Distance-constraint reachability computation in uncertain graphs. *Proc. VLDB Endow.* **4**(9), 551–562 (2011)
- [21] Lin, Y., Wan, H., Hu, J., Guo, S., Yang, B., Lin, Y., Jensen, C.S.: Origin-destination travel time oracle for map-based services. *arXiv preprint arXiv:2307.03048* (2023)
- [22] Yuan, H., Li, G., Bao, Z.: Route travel time estimation on A road network revisited: Heterogeneity, proximity, periodicity and dynamicity. *Proc. VLDB Endow.* **16**(3), 393–405 (2022)
- [23] Yuan, H., Li, G., Bao, Z., Feng, L.: Effective travel time estimation: When historical trajectories over road networks matter. In: *Proceedings of the International Conference on Management of Data, ACM, SIGMOD Conference, Online Conference [Portland, OR, USA]*, pp. 2135–2149 (2020)
- [24] Giannotti, F., Nanni, M., Pedreschi, D.: Efficient mining of temporally annotated sequences. In: *Proceedings of the Sixth SIAM International Conference on Data Mining, Bethesda, MD, USA*, pp. 348–359 (2006)
- [25] Asif, M.T., Dauwels, J., Goh, C.Y., Oran, A., Fathi, E., Xu, M., Dhanya, M.M., Mitrovic, N., Jaillet, P.: Spatiotemporal patterns in large-scale traffic speed prediction. *IEEE Trans. Intell. Transp. Syst.* (2), 794–804 (2014)
- [26] Morimoto, Y.: Mining frequent neighboring class sets in spatial databases. In: *Proceedings of the Seventh ACM SIGKDD International Conference on Knowledge Discovery and Data Mining, San Francisco, CA, USA*, pp. 353–358 (2001)
- [27] Zhang, X., Mamoulis, N., Cheung, D.W., Shou, Y.: Fast mining of spatial collocations. In: *Proceedings of the Tenth ACM SIGKDD International Conference on Knowledge Discovery and Data Mining, Seattle, Washington, USA*, pp. 384–393 (2004)
- [28] Yoo, J.S., Bow, M.: Mining top-k closed co-location patterns. In: *IEEE International Conference on Spatial Data Mining and Geographical Knowledge Services, ICSDM, Fuzhou, China*, pp. 100–105 (2011)
- [29] Yu, W.: Spatial co-location pattern mining for location-based services in road networks. *Expert Syst. Appl.*, 324–335 (2016)
- [30] Han, J., Pei, J., Yin, Y., Mao, R.: Mining frequent patterns without candidate generation: A frequent-pattern tree approach. *Data Min. Knowl. Discov.*, 53–87 (2004)

- [31] Kosyfaki, C., Mamoulis, N., Pitoura, E., Tsaparas, P.: Flow motifs in interaction networks. In: *Advances in Database Technology - 22nd International Conference on Extending Database Technology, EDBT, Lisbon, Portugal*, pp. 241–252 (2019)
- [32] Cai, J., Kwan, M.: Discovering co-location patterns in multivariate spatial flow data. *Int. J. Geogr. Inf. Sci.* **36**(4), 720–748 (2022)
- [33] Kosyfaki, C., Mamoulis, N., Pitoura, E., Tsaparas, P.: Flow computation in temporal interaction networks. In: *37th IEEE International Conference on Data Engineering, ICDE, Chania, Greece*, pp. 660–671 (2021)
- [34] Ansari, M.Y., Ahmad, A., Khan, S.S., Bhushan, G., Mainuddin: Spatiotemporal clustering: a review. *Artif. Intell. Rev.* **53**(4), 2381–2423 (2020)
- [35] Hadjieleftheriou, M., Kollios, G., Bakalov, P., Tsotras, V.J.: Complex spatio-temporal pattern queries. In: *Proceedings of the 31st International Conference on Very Large Data Bases, ACM, Trondheim, Norway*, pp. 877–888 (2005)
- [36] Zhang, J., Zheng, Y., Qi, D., Li, R., Yi, X., Li, T.: Predicting citywide crowd flows using deep spatio-temporal residual networks. *Artificial Intelligence* **259**, 147–166 (2018)
- [37] Paranjape, A., Benson, A.R., Leskovec, J.: Motifs in temporal networks. In: *Proceedings of the Tenth ACM International Conference on Web Search and Data Mining, WSDM, Cambridge, United Kingdom*, pp. 601–610 (2017)
- [38] La Barbera, A., Spagnolo, B.: Spatio-temporal patterns in population dynamics. *Physica A: Statistical Mechanics and its Applications* **314**(1-4), 120–124 (2002)
- [39] Tan, P.-N., Steinbach, M., Kumar, V., Potter, C., Klooster, S., Torregrosa, A.: Finding spatio-temporal patterns in earth science data. In: *KDD Workshop on Temporal Data Mining*, vol. 19 (2001)
- [40] Laube, P., Berg, M., Kreveld, M.J.: Spatial support and spatial confidence for spatial association rules. In: *Headway in Spatial Data Handling, 13th International Symposium on Spatial Data Handling, Springer, Montpellier, France. Lecture Notes in Geoinformation and Cartography*, pp. 575–593 (2008)
- [41] Mennis, J.L., Liu, J.W.: Mining association rules in spatio-temporal data: An analysis of urban socioeconomic and land cover change. *Trans. GIS*, 5–17 (2005)
- [42] Wang, J., Hsu, W., Lee, M.: A framework for mining topological patterns in spatio-temporal databases. In: *Proceedings of the ACM CIKM International Conference on Information and Knowledge Management, Bremen, Germany*, pp. 429–436 (2005)

- [43] Nanavati, A.A., Chitrapura, K.P., Joshi, S., Krishnapuram, R.: Mining generalised disjunctive association rules. In: Proceedings of the ACM CIKM International Conference on Information and Knowledge Management, Atlanta, Georgia, USA, pp. 482–489 (2001)
- [44] Zargari, S.A., Memarnejad, A., Mirzahosseini, H.: Hourly origin-destination matrix estimation using intelligent transportation systems data and deep learning. *Sensors* **21**(21), 7080 (2021)
- [45] Behara, K.N., Bhaskar, A., Chung, E.: Single-level approach to estimate origin-destination matrix: exploiting turning proportions and partial od flows. *Transportation Letters* **14**(7), 721–732 (2022)
- [46] Rong, C., Liu, Z., Ding, J., Li, Y.: Learning to generate temporal origin-destination flow based-on urban regional features and traffic information. *ACM Trans. Knowl. Discov. Data* **18**(6), 150–115017 (2024)
- [47] Xia, D., Jiang, S., Yang, N., Hu, Y., Li, Y., Li, H., Wang, L.: Discovering spatiotemporal characteristics of passenger travel with mobile trajectory big data. *Physica A: Statistical Mechanics and Its Applications* **578**, 126056 (2021)
- [48] Tu, P., Yao, W., Zhao, Z., Wang, P., Wu, S., Fang, Z.: Interday stability of taxi travel flow in urban areas. *ISPRS International Journal of Geo-Information* **11**(12), 590 (2022)
- [49] Pendyala, R.M., Goulias, K.G.: Time use and activity perspectives in travel behavior research. *Transportation* **29**(1), 1–4 (2002)
- [50] Djukic, T., Hoogendoorn, S., Van Lint, H.: Reliability assessment of dynamic od estimation methods based on structural similarity index. Technical report (2013)
- [51] Barceló, J., Ros-Roca, X., Montero, L.: Data analytics and models for understanding and predicting travel patterns in urban scenarios. In: *The Evolution of Travel Time Information Systems: The Role of Comprehensive Traffic Models and Improvements Towards Cooperative Driving Environments*, Springer, pp. 201–277 (2022)
- [52] Behara, K., Bhaskar, A.: Can partial structural information of travel demand improve the quality of od matrix estimates. In: *Proceedings of the Australasian Transport Research Forum, Brisbane, Australia*, pp. 8–10 (2021)
- [53] Chen, T., Nie, L., Pan, J., Tu, L., Zheng, B., Bai, X.: Origin-destination traffic prediction based on hybrid spatio-temporal network. In: *IEEE International Conference on Data Mining, ICDM, Orlando, FL, USA*, pp. 879–884 (2022)
- [54] Xian, X., Ye, H., Wang, X., Liu, K.: Spatiotemporal modeling and real-time prediction of origin-destination traffic demand. *Technometrics* **63**(1), 77–89

- (2021)
- [55] Xian, X., Ye, H., Wang, X., Liu, K.: Spatiotemporal modeling and real-time prediction of origin-destination traffic demand. *Technometrics* **63**(1), 77–89 (2021)
 - [56] Zou, X., Zhang, S., Zhang, C., James, J., Chung, E.: Long-term origin-destination demand prediction with graph deep learning. *IEEE Transactions on Big Data* **8**(6), 1481–1495 (2021)
 - [57] Hazelton, M.L.: Inference for origin–destination matrices: estimation, prediction and reconstruction. *Transportation Research Part B: Methodological* **35**(7), 667–676 (2001)
 - [58] Chu, K.-F., Lam, A.Y., Li, V.O.: Deep multi-scale convolutional lstm network for travel demand and origin-destination predictions. *IEEE Transactions on Intelligent Transportation Systems* **21**(8), 3219–3232 (2019)
 - [59] Behara, K.N., Bhaskar, A., Chung, E.: A dbscan-based framework to mine travel patterns from origin-destination matrices: Proof-of-concept on proxy static od from brisbane. *Transportation Research Part C: Emerging Technologies* **131**, 103370 (2021)
 - [60] Cao, H., Mamoulis, N., Cheung, D.W.: Mining frequent spatio-temporal sequential patterns. In: *Proceedings of the 5th IEEE International Conference on Data Mining (ICDM)*, Houston, Texas, USA, pp. 82–89 (2005)
 - [61] Kang, J., Yong, H.: Mining spatio-temporal patterns in trajectory data. *J. Inf. Process. Syst.* **6**(4), 521–536 (2010)
 - [62] Tao, Y., Faloutsos, C., Papadias, D., Liu, B.: Prediction and indexing of moving objects with unknown motion patterns. In: *Proceedings of the ACM SIGMOD International Conference on Management of Data*, pp. 611–622 (2004)
 - [63] Choi, D., Pei, J., Heinis, T.: Efficient mining of regional movement patterns in semantic trajectories. *Proc. VLDB Endow.* **10**(13), 2073–2084 (2017)
 - [64] Agrawal, R., Imielinski, T., Swami, A.N.: Mining association rules between sets of items in large databases. In: *Proceedings of the ACM SIGMOD International Conference on Management of Data*, Washington, DC, USA, pp. 207–216 (1993)
 - [65] Han, J., Fu, Y.: Mining multiple-level association rules in large databases. *IEEE Trans. Knowl. Data Eng.*, 798–804 (1999)
 - [66] Koperski, K., Han, J.: Discovery of spatial association rules in geographic information databases. In: *Advances in Spatial Databases, 4th International Symposium, SSD*, Portland, Maine, USA, Springer. *Lecture Notes in Computer Science*, pp.

- [67] Agrawal, R., Mannila, H., Srikant, R., Toivonen, H., Verkamo, A.I.: Fast discovery of association rules. In: *Advances in Knowledge Discovery and Data Mining*, AAAI/MIT Press, pp. 307–328 (1996)
- [68] Association rules, spatio-temporal. In: Shekhar, S., Xiong, H. (eds.) *Encyclopedia of GIS*, p. 32. Springer (2008). https://doi.org/10.1007/978-0-387-35973-1_76 . https://doi.org/10.1007/978-0-387-35973-1_76
- [69] Ye, J., Zhao, J., Zhang, L., Xu, C., Zhang, J., Ye, K.: A data-driven method for dynamic OD passenger flow matrix estimation in urban metro systems. In: *Big Data - BigData - 9th International Conference, Held as Part of the Services Conference Federation, SCF, Honolulu, HI, USA, Springer. Lecture Notes in Computer Science*, vol. 12402, pp. 116–126 (2020)
- [70] Pamula, T., Zochowska, R.: Estimation and prediction of the OD matrix in uncongested urban road network based on traffic flows using deep learning. *Eng. Appl. Artif. Intell.* **117**(Part), 105550 (2023)
- [71] Shi, H., Yao, Q., Guo, Q., Li, Y., Zhang, L., Ye, J., Li, Y., Liu, Y.: Predicting origin-destination flow via multi-perspective graph convolutional network. In: *36th IEEE International Conference on Data Engineering, ICDE, Dallas, TX, USA*, pp. 1818–1821 (2020)
- [72] Yu, P., Zhang, X., Gong, Y., Zhang, J., Sun, H., Zhang, J., Zhang, X., Yin, Y.: Enhancing origin-destination flow prediction via bi-directional spatio-temporal inference and interconnected feature evolution. *Expert Syst. Appl.* **264**, 125679 (2025)
- [73] Yung, K., Ying, J.J., Lin, H., Tseng, V.S.: Learning location semantics and dynamics for traffic origin-destination demand prediction. In: *International Joint Conference on Neural Networks, IEEE IJCNN, Yokohama, Japan*, pp. 1–8 (2024)
- [74] Gong, Y., Li, Z., Zhang, J., Liu, W., Zheng, Y.: Online spatio-temporal crowd flow distribution prediction for complex metro system. *IEEE Trans. Knowl. Data Eng.* **34**(2), 865–880 (2022)
- [75] Ashok, K.: Estimation and prediction of time-dependent origin-destination flows. PhD thesis, Massachusetts Institute of Technology (1996)
- [76] Ho, C., Agrawal, R., Megiddo, N., Srikant, R.: Range queries in OLAP data cubes. In: *SIGMOD, Proceedings ACM SIGMOD International Conference on Management of Data, Tucson, Arizona, USA*, pp. 73–88 (1997)